Responses of field-grown maize to different soil types, water regimes, and contrasting vapor pressure deficit

Thuy Huu Nguyen[1], Thomas Gaiser[1], Jan Vanderborght[3], Andrea Schnepf[3], Felix Bauer[3], Anja Klotzsche[3], Lena Lärm[3], Hubert Hüging[1], Frank Ewert[1, 2]

[1]University of Bonn, Institute of Crop Science and Resource Conservation (INRES), Katzenburgweg 5, 53115 Bonn, Germany

[2]Leibniz Centre for Agricultural Landscape Research (ZALF), Institute of Landscape Systems Analysis, Eberswalder Strasse 84, 15374 Muencheberg, Germany

[3]Agrosphere (IBG-3), Institute of Bio- and Geosciences, Forschungszentrum Jülich GmbH, 52428, Jülich, Germany

[*]Corresponding author, email: tngu@uni-bonn.de

Abstracts

Drought is a serious constraint to crop growth and production of important staple crops such as maize. Improved understanding of the responses of crops to drought can be incorporated into cropping system models to support crop breeding, varietal selection and management decisions for minimizing negative impacts. We investigate the impacts of different soil types (stony and silty) and water regimes (irrigated and rainfed) on hydraulic linkages between soil and plant, as well as root: shoot growth characteristics. Our analysis is based on a comprehensive dataset measured along the soil-plant-atmosphere pathway at field scale in two growing seasons (2017, 2018) with contrasting climatic conditions (low and high VPD). Roots were observed mostly in the topsoil (10-20 cm) of the stony soil while more roots were found in the subsoil (60-80 cm) of the silty soil. The difference in root length was pronounced at silking and harvest between the soil types. Total root length was 2.5 - 6 times higher in the silty soil compared to the stony soil with the same water treatment. At silking time, the ratios of root length to shoot biomass in the rainfed

24 plot of the silty soil (F2P2) were 3 times higher than those in the irrigated silty soil (F2P3) while the ratio

25 was similar for two water treatments in the stony soil. With the same water treatment, the ratios of root

26 length to shoot biomass of silty soil was higher than stony soil. The seasonally observed minimum leaf

27 water potential (ψ_{leaf}) varied from around -1.5 MPa in the rainfed plot in 2017 to around -2.5 MPa in the

28 same plot of the stony soil in 2018. In the rainfed plot, the mimimum ψ_{leaf} in the stony soil was lower than

29 in silty soil from -2 to -1.5 MPa in 2017, respectively while these were from -2.5 to -2 MPa in 2018,

30 respectively. Leaf water potential, water potential gradients from soil to plant roots, plant hydraulic

31 conductance (K_{soil_plant}), stomatal conductance, transpiration, and photosynthesis were considerably

32 modulated by the soil water content and the conductivity of the rhizosphere. When the stony soil and silt

33 soil are compared, the higher 'stress' due to the lower water availability in the stony soil resulted in less

34 roots with a higher root tissue conductance in the soil with more stress. When comparing the rainfed with

35 the irrigated plot in the silty soil, the higher stress in the rainfed soil resulted in more roots with a lower

36 root tissue conductance in the treatment with more stress. This illustrates that the 'response' to stress can

37 be completely opposite depending on conditions or treatments that lead to the differences in stress that

38 are compared. To respond to water deficit, maize had higher water uptake rate per unit root length and

39 higher root segment conductance in the stony soil than in the silty soil, while the crop reduced transpired

40 water via reduced aboveground plant size. Future improvements of soil-crop models in simulating gas

41 exchange and crop growth should further emphasize the role of soil textures on stomatal function,

42 dynamic root growth, and plant hydraulic system together with aboveground leaf area adjustments.

43 **Key words:** irrigation, plant hydraulic conductance, transpiration, root length, soil types, soil to leaf water

44 potential, stomatal regulation

45 **Abbreviations:** DOY: day of the year; DAS: day after sowing; TUE: transpiration use efficiency; SF: sap flow;

46 LAI: green leaf area index; PAR: photosynthetically active radiation; VPD: vapor pressure deficit; An: net

47 leaf photosynthesis; E: leaf transpiration; ψ_{leaf}: leaf water potential; $\psi_{sunlitleaf}$: leaf water potential of sunlit

48   leaf; $\psi_{shadedleaf}$: leaf water potential of shaded leaf; K_{soil}: hydraulic conductance of soil; K_{root}: root hydraulic

49   conductance; K_{stem}: stem hydraulic conductance; ψ_{soil_effec}: effective soil water potential; $\psi_{difference}$:

50   difference between effective soil water potential and sunlit leaf water potential; K_{soil_root}: root system

51   hydraulic conductance (includes soil and root hydraulic conductance); K_{soil_plant}: whole plant hydraulic

52   conductance (includes below and aboveground components).

53   **1. Introduction**

54   Maize (*Zea mays L.*) is a major staple crop throughout the world. Drought stress, which negatively affects

55   crop growth and yield, is of increasing concern in several important maize cultivating regions (Daryanto et

56   al., 2016). Increases in frequency and severity of drought events due to climate change have been recently

57   reported (IPCC, 2022). Thus, field observations and understanding on how maize responds to water stress

58   are necessary to suggest promising traits for breeding programs (Vadez et al., 2021) as well as irrigation

59   schemes (Fang and Su, 2019; Q. Cai et al., 2017). Improved understanding of crops' response to drought

60   can be incorporated into soil-crop models (e.g. crop modelling and soil-vegetation-atmosphere transfer

61   modelling).

62   Stomatal regulation is often considered as a key aboveground hydraulic variable in regulating water use

63   of crops. Maize is known as an isohydric plant. Maize stomata are closed in response to drought conditions

64   to maintain leaf water potential (ψ_{leaf}) above critical levels ($\psi_{threshold}$ or minimum ψ_{leaf}) (Tardieu and

65   Simonneau, 1998). The isohydric behavior is due to different mechanisms including hydraulic and/or

66   chemical (e.g. abscisic acid [ABA]) signals (Tardieu, 2016). The degree to which these underlying

67   mechanisms interact and differ among genotypes and/or environmental scenarios in explaining the

68   stomatal regulation is still debated (Tardieu, 2016, Hochberg et al., 2018). Field evidence in variation of

69   the minimum ψ_{leaf} of maize due to soil water availability and soil hydraulics is rarely reported.

70   Water flow along the soil-plant-atmosphere continuum is determined by a series of hydraulic

71   conductivities and gradients in water potential. Hydraulic conductance of soil (K_{soil}), root hydraulic

72 conductance (K_{root}), and stem hydraulic conductance (K_{stem}) determine water potential from soil to root

73 and root xylem water, and thus magnitude of ψ_{leaf}. There are two main resistances to water flow from the

74 soil to the shoot, namely the soil and the root resistances, often expressed as their inverse, K_{soil} and K_{root}

75 (Nguyen et al., 2020; Cai et al., 2018). In wet soils, the soil hydraulic conductivity is much higher than that

76 of roots, and water flow is mainly controlled by root hydraulic conductivity (Hopmans and Bristow, 2002;

77 Draye et al., 2010). It is well-known that a decrease in soil matric potential and soil hydraulic conductivity

78 triggers stomatal closure and thus results in reduction in transpiration rate (Sinclair and Ludlow, 1986;

79 Carminati and Javaux 2020; Abdalla et al., 2021). For the root water uptake and controlling stomata, the

80 location where soil and roots are in close contact (rhizosphere) is most important, because when this thin

81 layer of rhizosphere is disconnected (i.e. soil-root contact is lost), the water movement from soil toward

82 the roots is reduced, which might trigger stomatal closure to maintain hydraulic integrity of plant

83 (Carminati et al., 2016; Rodriguez-Dominguez and Brodribb, 2019; Abdalla et al., 2022). The magnitude of

84 the drop of water potential between bulk soil and soil-root interface increases considerably at different

85 levels of soil dryness for different soil types (Carminati and Javaux, 2020; Abdalla et al., 2022). Hydraulic

86 limits in the soil (Carminati and Javaux, 2020), or in the root–soil interface [as measured for olive trees by

87 Rodriguez-Dominguez and Brodribb, 2019 or tomato (Abdalla et al., 2022)], or in the root properties

88 (Bourbia et al., 2021; Cai et al., 2022; Nguyen et al., 2020; Cai et al., 2018) or due to both soil textures and

89 root phenotypes (Cai et al., 2022b) emphasized the importance of belowground hydraulics (Carminati and

90 Javaux, 2020). However, also the shoot hydraulic conductance could be limiting in some crop plants

91 (Gallardo et al., 1996) or in trees (Domec and Pruyn, 2008; Tsuda and Tyree, 1997). Stomatal conductance

92 and shoot hydraulic conductance showed close links to each other in pine trees (Hubbard et al., 2001).

93 This summary illustrates three points: (i) current studies have often focused either on above or on below

94 hydraulic limits, but rarely consider both (ii) the roles and relations of soil hydraulic properties to root and

95 plant hydraulic conductance (thus influences on stomatal conductance) remain unclear (iii) the role of

96   different hydraulic processes across the soil - plant - atmosphere continuum i.e. soil to roots, stem, and

97   soil-plant hydraulic conductance in controlling stomatal conductance remains unclear.

98   Simultaneous measurements of atmospheric conditions (light intensity and vapor pressure deficit), leaf

99   water potential, and transpiration rates, coupled with measurements of root, stem and whole soil-plant

100   hydraulic conductance, root architecture, and soil water potential distribution could reveal the relative

101   importance of rhizosphere, shoot and root growth, and hydraulic conductance vulnerability, especially

102   under progressive soil drying at field conditions (Carminati and Javaux, 2020; Tardieu et al., 2017). For the

103   soil water conditions, soil texture and hydraulic characteristics are very important because they influence

104   soil water movement and thus affect infiltration, surface and sub-surface runoff, and ultimately plant

105   available soil water (Vereecken et al., 2016). Soil texture properties, characterized by different fractions of

106   clay, silt, and sand particles, are important drivers in determining the soil water retention properties

107   (Scharwies and Dinneny, 2019; Stadler et al., 2015; Zhuang et al., 2001). Soil with higher water holding

108   capacity (here the silty soil with low stone content) have a larger amount of plant available water which in

109   turn enables crops to better meet the evaporative demand and facilitates better crop growth as compared

110   to the soil with high stone content (Nguyen et al., 2020; Cai et al., 2018). Estimations of hydraulic

111   conductance (different organs and whole plant hydraulic conductance) were done for crop plants and

112   maize mainly under controlled environment or pot conditions e.g. for different species and genotypes

113   during soil drying (Sunita et al., 2014; Choudhary and Sinclair, 2014; Abdalla et al., 2022; Meunier et al.,

114   2018; Wang et al., 2017; Li et al., 2016) or various species and genotypes together with different soil

115   textures (Cai et al., 2022a), or soil texture with different vapor pressure deficit (VPD) (Cai et al., 2022b).

116   Compared to the substantial effect of soil texture, there was no evidence of an effect of VPD on both soil–

117   plant hydraulic conductance and on the relation between canopy stomatal conductance and soil–plant

118   hydraulic conductance in pot-grown maize (Cai et al., 2022b). Contrast results were found in winter wheat

119   where plant hydraulic conductance increased with rising VPD for some genotypes in wet conditions

120 (Ranawana et al., 2021). Vadez et al., (2021) examined the effects of soil types together with increasing

121 VPD on transpiration efficiency (TE) and yield under pot conditions for several C_4 species (maize, sorghum,

122 and millet). The interpretation of differences in TE was attributed to soil types, more specifically, to the

123 differences in soil hydraulic properties and soil hydraulic conductance. However, experimental evidence

124 linking root hydraulics to stomatal regulation was lacking in these two Vadez's studies (Vadez et al., 2021).

125 Recent field studies have aimed at quantification of root hydraulic conductance and it's linkages with crop

126 growth (leaf area and biomass) under different soil types (in wheat Cai et al., 2017; Cai et al., 2018; Nguyen

127 et al., 2020 or maize in Nguyen et al., 2022; Jorda et al., 2022). However, field studies that consider both

128 below (soil-root hydraulic conductance) and above (stem hydraulic conductance), or soil-plant hydraulic

129 conductance (including below and above-ground parts) and their roles in stomatal regulation as well as

130 crop growth (leaf area and biomass) are rarely carried out.

131 This study aims at further understanding of the hydraulic linkages between soil and plant and responses

132 of plants to drought stress in relation to root: shoot growth characteristics at field scale. We hypothesize

133 that, in field-grown maize, (1) soil-plant hydraulic conductance depends on soil hydraulic properties,

134 especially under dry soil conditions (2) minimum leaf water potential of maize is similar across soil types,

135 water treatments and climatic conditions. The hypotheses will be tested through three objectives: (i) to

136 investigate the effects of soil types, water application, and climatic condition on root growth and (ii) on

137 stomatal conductance, leaf photosynthesis, transpiration, leaf water potential, different components of

138 the hydraulic conductance (root, stem, and whole soil-plant), and (iii) to analyze the relative contribution

139 of root and shoot growth (leaf area and biomass) on the water uptake capacity of maize. These three

140 objectives will be achieved based on a comprehensive dataset covering the whole soil-plant continuum

141 over two growing maize seasons with contrasting climatic conditions (low and high VPD) under two water

142 treatments (rainfed and irrigated) and two different soil types (stony and silty soil).

143

2. Materials and methods

2.1. Location and experimental set-up

We carried out a field experiment at two rhizotron facilities in Selhausen, North Rhine-Westphalia, Germany (50°52'N, 6°27'E). The field is slightly inclined with a maximum slope of around 4. One rhizotrone facility was located upslope (F1) with around 60% gravel by weight in the 10-cm topsoil while the second rhizotrone facility was at downslope (F2) with silty soil (stone content is around 4% by weight).

Each rhizotrone facility was divided into three subplots of 7.25 m by 3.25 m: two rainfed plots (P1, P2), and one irrigated plot (P3). In rainfed plots P1, other sowing densities and dates were used than in the other plots and we excluded therefore these plots. Silage maize *cv.* Zoey was sown on 4 May and 8 May in 2017 and 2018, respectively, with a plant density of 10.66 seeds m^{-2} (Figure 1a; Table 1). Detailed information of crop management practices is provided in Table 1.

[Insert Table 1 here]

2.2. Water applications

The irrigation systems [T-Tape 520-20-500 drip lines (Wurzelwasser GbR, Müzenberg, Germany)] were installed parallel to the crop rows with 0.3 m intervals. A nearby weather station (approx. 100 m from the experiment) recorded every 10 minutes weather variables (global radiation, temperature, relative humidity, precipitation, and wind speed). In addition, the precipitation amount was manually collected by a plastic rain gauge next to each rhizotrone facility. The Penman-Monteith equation was employed to estimate reference evapotranspiration. Daily crop evapotranspiration was calculated based on the single crop coefficient and the reference evapotranspiration (Allen et al., 1998). Irrigation amounts were estimated as the weekly sum of the calculated crop evapotranspiration. A total amount of 230 mm precipitation was recorded during the growing period (136 days) while average, minimum and maximum daily air temperature were 17.6, 8.3, and 25.3 °C, respectively (Fig. 1b). The crop on the irrigated plots (2017F1P3 and 2017F2P3) was received in total 130 mm (10 times, every 5-7 days, using 13 mm of

168   irrigation water per event) between mid June to end of August (Fig. 1b). Average, minimum, and maximum

169   daily air temperature in 2018 were higher than in 2017 with 19.2, 10.85, and 27.3 °C, respectively (Fig. 1b).

170   The summer season in 2018 could be considered as an extreme year with respect to plant growth at our

171   experimental location due to exceptionally hot and dry weather conditions. Crop received only 91.3 mm

172   of rain during the growing period of 2018 (107 days). The crop on the irrigated plots 2018F1P3 and

173   2018F2P3 was irrigated every 5-7 days (in total 13 times), with a total amount of irrigation of 257 mm and

174   239 mm between mid- June and mid- August, respectively (Fig. 1d). To avoid a crop failure due to severe

175   drought in 2018, the rainfed plot in the stony soil (2018F1P2) had to be irrigated (in total 66 mm) four

176   times (using 13, 22, 13, and 18 mm, respectively) (Fig. 1d). Detailed estimates of irrigation amount and

177   intervals could be found in Nguyen et al., (2022a).

178   [Insert Figure 1 here]

179   **2.3. Measurements**

180   **2.3.1. Soil water measurement and root growth**

181   MPS-2 matrix water potential and temperature sensors (Decagon Devices Inc., UMS GmbH München,

182   Germany) were installed at soil depths of 10, 20, 40, 60, 80, and 120 cm to measure half-hourly soil water

183   potential and soil temperature. The range of the water potential measurements is from -9 kPa to

184   approximately -100000 kPa (pF 1.96 to pF 6.01). In addition to MPS-2, soil water potential was measured

185   by pressure transducer tensiometers (T4e, UMS GmbH, München, Germany) where the minimum

186   detectable suction is -85 kPa to +100 kPa. A detailed description of sensor installation, calibration and data

187   post processing can be found in Cai et al., (2016).

188   Minirhizotubes (7 m long clear acrylic glass tubes with outer and inner diameters of 6.4 and 5.6 cm,

189   respectively) were installed horizontally at six different depths of 10, 20, 40, 60, 80, and 120 cm below the

190   soil surface in each facility. There are three replicate tubes at each depth, accounting for 54 tubes in each

191 facility. Root measurements were taken manually by Bartz camera (Bartz Technology Corporation) (23

192 June 2017 – 12 September2017) and VSI camera (Vienna Scientific Instruments GmbH) (08 June 2017 – 22

193 June 2017) in 2017 while only VSI was used in 2018 (23 May2018 - 23 August 2018). Root images were

194 taken at 20 fixed positions from the left- and right-hand sides of each tube weekly (or biweekly) during the

195 growing seasons. The root images were analyzed by automated minirhizotube image analysis pipeline for

196 segmentation and automated feature extraction (Bauer et al., 2021). Two-dimensional root length density

197 (RLD, in units of cm cm^{-2}) was estimated from the total root length observed in the image and the image

198 surface area. The overview of camera system, minirhizotube images acquisition, and post-processing of

199 the root data were described in detail in Bauer et al. (2021) and Lärm et al., (2023).

200 **2.3.2. Crop growth**, **leaf gas exchange, leaf water potential, and sap flow measurements**

201 The phenology, plant height, stem diameter, green and brown leaf area, dry matter of different organs,

202 and total aboveground dry matter were observed and measured bi-weekly. Dates of sowing, emergence,

203 tasseling, and silking for two growing seasons were observed. There was difference in emergence,

204 tasseling and silking dates for two growing seasons due to the differences of sowing dates and

205 temperature. However, the developmental stages were not different among water treatments and soil

206 types within one season. Measurements of green leaf area and aboveground dry matter were based on

207 the destructive method.

208 We performed leaf gas measurements under clear sky and sunny conditions. Hourly leaf stomatal

209 conductance (Gs), net photosynthesis (An), and leaf transpiration (E) of two sunlit leaves (uppermost fully

210 developed leaves) and one shaded leaf of different plants were measured every two weeks. The Gs, An,

211 and E were measured at steady-state using a LICOR 6400 XT device (Licor Biosciences, Lincoln, Nebraska,

212 USA). Leaf water potential (ψ_{leaf}) was measured with a pressure chamber (SKPM 140/ (40-50-80), Skye

213 Instrument Ltd, UK).

214   Based on stem diameter size, twenty sap flow sensors (SGA 13, SGB 16, and SGB 19 types) were installed

215   (one sensor per plant and 5 maize plants per treatment) in each year. The sensors were operated from 7

216   July 2017 and from 28 June 2018 until harvest for the 2017 and 2018 growing season, respectively. The

217   calculated sap flow in the plant (g h^{-1}) from the data loggers (Dynamax, 2007) was used to compute canopy

218   transpiration based on the plant density per square meter. Further detail of developmental stages, crop

219   growth, leaf gas exchange, leaf water potential, and sap flow measurements could be found in Nguyen et

220   al., (2024), Nguyen et al., (2022a) and Nguyen et al., (2020).

221   **2.4. Calculation of total root length, root system conductance, stem, and whole plant hydraulic**

222   **conductance**

223   To estimate the total root length from minirhizotubes, we adopted the option 2 which was described in

224   Cai et al., (2017). Total root length per square meter soil surface area within each soil layer (m m^{-2}) was

225   computed by multiplying the root length density with the corresponding soil layer thickness. The root

226   length density was determined in each depth by dividing the measured root length per minirhizotron

227   image by the assumed volume the roots would have occupied in absence of the tube, i.e., W * L * tube

228   radius (see Cai et al., 2017).

229   Following Nguyen et al., (2020), the effective soil water potential was calculated based on hourly measured

230   soil water potential (ψ_i) and normalized root length density at six depths (10, 20, 40, 60, 80, and 120 cm)

231   (NRLD$_i$), and soil layer thickness (Δz_i) in the soil profile (Equation 1).

$$\psi_{soil\_effec} = \sum_{i=1}^{N} \psi_i NRLD_i \, \Delta z_i \tag{1}$$

232   We followed Ohm's law analogy by dividing the hourly sap flow by the difference between effective soil

233   water potential and shaded leaf water potential to estimate root system conductance (K$_{soil\_root}$ - Equation

234   2), between shaded leaf water potential and sunlit leaf water potential to estimate stem hydraulic

235 conductance (K_{stem} - Equation 3), and between effective soil water potential and sunlit leaf water potential

236 to estimate whole plant hydraulic conductance (K_{soil_plant} - Equation 4).

$$K_{soil\_root} = Sapflow/(\psi_{soil\_effec} - \psi_{shadedleaf}) \tag{2}$$

$$K_{stem} = Sapflow/(\psi_{shadedleaf} - \psi_{sunlitleaf}) \tag{3}$$

$$K_{soil\_plant} = Sapflow/(\psi_{soil\_effec} - \psi_{sunlitleaf}) \tag{4}$$

237 During one measurement day, four values of the K_{soil_root}, K_{stem}, and K_{soil_plant} were obtained from

238 measurements between 11AM and 2 PM. The average and standard deviation of these hourly

239 measurements were calculated for each measurement day in order to present the seasonal dynamics of

240 those variables. To capture the diurnal and seasonal variations of sap flow and sunlit leaf water potential,

241 in addition, we plotted the hourly sap flow and hourly difference of effective soil water potential and sunlit

242 leaf water potential for three measurement days starting from predawn and whole seasons, respectively,

243 to derive the slope which is also K_{soil_plant}.

244 **2.5. Statistical analysis**
245

246 Regression analysis was performed to understand the relationship between the sap flow volume and the

247 difference of effective soil water potential and sunlit leaf water potential as well as the relationship

248 between the total aboveground biomass and cumulated water transpired (sap flow volume). These

249 analyses allow to derive the slope as proxy of K_{soil_plant} and transpiration use efficiency, respectively. Since

250 all measured data have their own measurement errors, the generalized Deming regression was employed.

251 We performed relationships (via correlation coefficient and statistical significant levels) of midday An,

252 Gs, and E with midday K_{stem}, K_{soil_plant}, K_{soil_root}, sunlit leaf potential, ψ_{soil_effec}, and the difference of ψ_{soil_effec}

253 and sunlit leaf water potential ($\psi_{difference}$). All data processing and analysis were conducted using the R

254 statistical software (R Core Team, 2022).

255 **3. Results**

3.1. Root growth under different water treatments, soil types and climatic conditions

Observed root length (cm cm^{-2}) from the minirhizotubes in different soil depths at the first week of June (stem elongation), around silking, and at harvest in two growing seasons are shown in the Figure 2. Root length was similar among water treatments at the start of stem elongation in both years (Fig. 2a & 2d). The difference in root length was pronounced at silking and harvest between the soil types. More root growth was observed in the silty soil compared to the stony soil with the same water treatment (i.e. 2.5 - 6 times higher at depth 40 cm). This indicated the strong negative effects of stone content on root development. In the stony soil, root length in the irrigated plot (F1P3) was slightly higher than in the rainfed plot (F1P2). In contrast, the rainfed treatment (F2P2) in the silty soil showed much higher root length, especially from 40 to 120 cm depths as compared to the irrigated plot (F2P3) in both growing seasons. Much lower stone content and deep soil cracks in the silty soil (Morandage et al., 2021) allow root extension to the subsoil, particularly in the rainfed plot F2P2. Root length in the rainfed treatment (F2P2) in 2018, is higher than in 2017 which implies that root further developed to exploit the water in the soil under the rainfed condition to meet the higher evaporative demand.

[Insert Figure 2 here]

Total root length (m m^{-2}) estimated from minirhizotubes and its ratio to shoot dry matter (m kg^{-1}) at three measured dates (as in Figure 2) are shown in the Figure 3. Total root length was much higher for the silty plots as compared to stony plots. In 2017, the highest total root length was observed in the rainfed plot of the silty soil (F2P2) with approximately 9166 m m^{-2} and 9878 m m^{-2} around silking and harvest, respectively, which was almost two times higher than in the irrigated plot (F2P3). These figures were higher in 2018 than 2017 where total root length of F2P2 was 10188 m m^{-2} and 13750 m m^{-2} at silking and harvest time, respectively. For the rainfed stony soil (F1P2), soil water depletion around the beginning of June in 2017 (Figure S1a) and from the first two weeks of June to harvest in 2018 (Figure S2a) caused the strong reduction of shoot biomass. In the stony soil, the shoot dry matter of the irrigated plot (F1P3) and the

280   rainfed plot (F1P2) were 1275 and 536 g m^{-2} at silking time (e.g. 19 July 2018 – DOY 200, Figure S3a and

281   S3b). However, there was a minor difference between F1P2 and F1P3 in terms of the ratio of root length

282   to shoot dry matter. In the silty soil, a decrease of soil water potential was not pronounced (compared to

283   stony soil) in both years 2017 and 2018 (Figure S1b and S2b). In 2018, shoot biomass in the irrigated stony

284   soil (F1P3) and silt soil (F2P3) were similar (1275 and 1299 g m^{-2}, respectively on 19 July 2018 – DOY 200)

285   while the shoot biomass of the rainfed silty soil (F2P2) was 876 g m^{-2} (Figure S3a & S3b). However, the

286   ratios of root length to shoot biomass in the rainfed plot of the silty soil (F2P2) were 3 and 6 times higher

287   than those in the irrigated silty soil (F2P3) and stony soil (F1P3), respectively (e.g. 18 July, DOY 199).

288   Moreover, total root length was relatively equal among treatments at the start of set elongation (8 June -

289   DOY 159) in both years, while this was the opposite for the ratio of root length to shoot dry matter. This

290   firstly illustrated that the finer soil texture without stones and with soil cracks could favor the root growth

291   which indicates strong interactions of root and soil conditions. Secondly, the larger root length and higher

292   atmospheric evaporative demand in 2018 than 2017 indicates also the interaction of root growth and

293   climatic conditions.

294   [Insert Figure 3 here]

295   **3.2. Stomatal conductance, photosynthesis, transpiration, and K$_{soil\_plant}$**

296   **3.2.1. Diurnal course of stomatal conductance, photosynthesis, transpiration, and water potential at leaf**

297   **level**

298   After a long period with high temperatures and no rainfall, soil water reduction in the rainfed plot of the

299   stony soil (F1P2) on 17 July 2018 (Figure S2) resulted in three times lower net photosynthesis (An),

300   stomatal conductance (Gs), transpiration (E) and leaf water potential (ψ_{leaf}) as compared to the remaining

301   treatments (Figure S4). This indicates that the soil water content strongly affected the stomatal

302   conductance. Stomatal closure was much pronounced around midday in F1P2 while this was not the case

303   in the F2P2, indicating the soil type strongly affected the stomatal conductance and leaf gas exchange.

304 Leaf gas exchange and leaf water potential in the F1P2 were still much lower than in other plots (Figure

305 4). On 18 July 2018, after application of 22.75 mm of irrigation water (at 4 PM), photosynthesis, stomatal

306 conductance, transpiration and leaf water potential were slightly increased in F1P2. However, these were

307 still smaller than in F2P2 and the two irrigated plots.

308 [Insert Figure 4 here]

309 On the next day after irrigation, leaf gas exchange and water potential were considerably increased in the

310 F1P2 (Figure S5). Leaf curling was also less pronounced as compared the two previous days. Predawn and

311 midday leaf water potential were around -0.4 MPa and -1.6 MPa for all plots, respectively. Leaf

312 transpiration rate was around 3.1 millimole m^{-2} s^{-1} for all water treatments and soil types at 12 AM. This

313 indicated the recovery of plant after watering at the rainfed plot with stony soil (F1P2).

314 **3.2.2. Seasonal course of stomatal conductance, photosynthesis, transpiration, water potential, and**

315 **plant hydraulic conductance at the leaf level**

316 Seasonal stomatal conductance (Gs) and leaf water potential (ψ_{leaf}) are described in Figure 5. The

317 relationship between two variables was rather noisy and non-linear. The leaf water potential showed

318 distinct patterns among treatments in one growing season. Minimum ψ_{leaf} was maintained at around -1.5

319 MPa in the irrigated plot in stony soil (F1P3) and two plots in the silty soil (F2P2 and F2P3). Lower minimum

320 ψ_{leaf} could be observed in the rainfed plot with stony soil (F1P2) but it did not go beyond -2 MPa. Minor

321 leaf curling was observed only in the second week of June in the F1P2 in 2017. In 2018, the higher

322 temperature and vapor pressure deficit resulted in lower minimum ψ_{leaf} in all treatments and soil types as

323 compared to 2017. The minimum ψ_{leaf} was around -2 MPa in F1P3, F2P2, and F2P3 while ψ_{leaf} could drop

324 below -2 MPa in F1P2 which was due to the severe soil water deficit. The low Gs and ψ_{leaf} associated with

325 measurement dates when the substantial leaf curling was observed at mid of July to the end of growing

326 season in F1P2 in 2018 (Figure S3c & S3d and Figure S6c & d).

327   [Insert Figure 5 here]

328   The effective soil water potential ($\psi_{soil\_effect\ MD}$), sunlit leaf water potential ($\psi_{sunlitleaf\ MD}$), stomatal

329   conductance (Gs_{MD}), and whole plant hydraulic conductance ($K_{soil\_plant\ MD}$) at midday at several times during

330   the growing season are presented in Figures 6 and 7 for 2017 and 2018, respectively. As expected, there

331   was not much difference in terms of $\psi_{soil\_effecMD}$ among F1P3, F2P2, and F2P3 from 02 August to one week

332   before harvest in 2017. The lowest $\psi_{soil\_effec\ MD}$ was observed in the F1P2. Leaf water potential dropped

333   drastically but also $K_{soil\_plant\ MD}$ increased strongly whereas $\psi_{soil\_effec\ MD}$ remained quite similar (e.g. 18 July).

334   This is because sap flow have increased substantially in this day (e.g. from 2.34 mm d^{-1} on 17 July to 6.97

335   mm d^{-1} on 18 July for the F1P2). The stomatal conductance decreased a lot in this day which could be

336   explained that the atmospheric demand increased (e.g. global radiation was 13.6 MJ m^{-2} on 17 July

337   compared to 23.9 MJ on 18 July while daily VPD was 0.7 kPa and 1.2 kPa, respectively) even more than the

338   sap flow. Midday sunlit leaf water potential was not distinctively different among treatments with the

339   lowest $\psi_{sunlitleaf\ MD}$ around -1.6 MPa throughout season. Also, Gs_{MD} was rather similar among plots. The

340    $K_{soil\_plant\ MD}$ ranged from 0.125 to 0.96 mm h^{-1} MPa^{-1} with a sharp reduction before harvest. In general, the

341   lowest values of $K_{soil\_plant\ MD}$ were found in F1P2 which was consistent with the smaller overall seasonal

342   K_{soil_plant} (as the slope of linear relationship between sap flow and difference of effective soil water potential

343   and sunlit leaf water potential) (see Figure S7).

344   [Insert Figure 6 here]

345   The $\psi_{soil\_effec\ MD}$ was substantially different in the two soil types and water treatments in 2018 (Figure 7a).

346   Both F1P2 and F1P3 showed a gradual drop of $\psi_{soil\_effec\ MD}$ from 15 June until the third week of July then

347   increased after irrigation events on 18 July (Figure S2b). However, $\psi_{soil\_effec\ MD}$ of F1P2 was much lower than

348   F1P3 toward the harvest. The $\psi_{soil\_effec\ MD}$ of F2P2 and F2P3 only decreased progressively from around 10

349   July till harvest even though there was water supply from the irrigation (Figure S2b). The water applied by

350 irrigation and coming in by rainfall were insufficient to wet up the deeper soil layers which remained dry.

351 The low Gs_{MD} was corresponding to the lowest $\psi_{sunlitleaf\ MD}$ and $K_{soil\_plant\ MD}$ from the F1P2 (Figure 7c & 7d).

352 The $K_{soil\_plant\ MD}$ from all plots was ranging from 0.12 to 0.91 mm h^{-1} MPa^{-1}. There was the drop in $K_{soil\_plant\ MD}$

353 (i.e. 3 to 9 July or 17-18 July) before irrigation in this plot. However, it increased after the irrigation (i.e. 10

354 July and 19 July). This suggests that K_{soil_plant} depends strongly on the soil water content and the

355 conductivity of the rhizosphere.

356 [Insert Figure 7 here]

357 **3.2.3. Relationships of stomatal conductance, transpiration, photosynthesis with plant hydraulic**

358 **variables at the plant canopy level**

359 The slope of linear relationship between sap flow and difference of ψ_{soil_effec} and $\psi_{sunlitleaf}$ is shown for three

360 consecutive days (leaf water potential measurements from the predawn) and before and after irrigation

361 applications (17, 18, and 19 July 2018) (Figure 8). On both dates 17 and 18 July, the difference between

362 ψ_{soil_effec} and $\psi_{sunlitleaf}$ was around -1.6 MPa with very low transpiration rates in the treatment F1P2 which

363 was associated with very low plant hydraulic conductance and leaf curling. The whole plant hydraulic

364 conductance was disrupted on these two days (0.06 and 0.16 mm h^{-1} MPa^{-1} for 17 and 18 July, respectively).

365 Water was supplied on 18 July at 1 PM for the irrigated plots (F1P3, F2P3) as well as F1P2 at 4 PM (for

366 saving plant from death due to severe drought stress). K_{soil_plant} was slightly changed (0.43 and 0.57 mm h^{-1}

367 ^{1} MPa^{-1} for F1P3 on 18 and 19 July, respectively and 0.5 and 0.58 mm h^{-1} MPa^{-1} for F2P3 on 18 and 19 July,

368 respectively). However, the increase of K_{soil_plant} was substantial in the F1P2 after the irrigation. Soil water

369 replenishment and an increase in the root - soil contact (Fig. 7a) allowed the K_{soil_plant} to recover overnight

370 to 0.46 mm h^{-1} MPa^{-1}. This resulted in a narrower water potential gradient between root zone and sunlit

371 leaf and in a higher transpiration rate on 19 July.

372 [Insert Figure 8 here]

373 Seasonal average of different midday hydraulic conductance components (root system hydraulic

374 conductance - K_{soil_root}, stem hydraulic conductance – K_{stem}, and whole plant hydraulic conductance –

375 K_{soil_plant}) are shown in Figure 9. In the same year, the K_{stem} was not much different among F1P3, F2P2, and

376 F2P3 plots. The K_{stem} of those plots was slightly higher than in the F1P2 in both years. In general, the K_{soil_root}

377 was lower than the K_{stem}. Overall, the estimated K_{soil_plant} was around $1/(1/K_{soil\_root} +1/K_{stem})$ regardless of

378 soil types, years, and water treatments. The K_{soil_root} and K_{soil_plant} in the F1P2 in 2018 was much lower than

379 the remaining plots while the K_{soil_root} and K_{soil_plant} were not much different among plots in 2017. Our results

380 indicated that there was an impact of soil hydraulic conductance on K_{soil_root} and K_{soil_plant}. Although there is

381 a large difference in total root length between the two soil types (e.g. F1P3 versus F2P2 or F2P3 versus

382 F2P2), K_{soil_root} and K_{soil_plant} in those two plots were not much different. This could be explained by the fact

383 that K_{soil_plant} was not only depended on root length but also depended on the variability of root segment

384 hydraulic conductance.

385 [Insert Figure 9 here]

386 **3.3. Relative importance of root and leaf area growth to transpiration and crop performance at canopy**

387   **level**

388 Drought stress was observed in the rainfed plot (F2P2) in the second week of June 2017 with mild leaf

389 rolling. The crop then recovered due to sufficient rainfall and lower evaporative demand. Drought stress

390 occurring again at the stem elongation phase caused reduction of plant size (height and stem diameter)

391 (Figure S6) as well as a slight reduction of leaf area and biomass in this plot (Figure S3a & S3c). Transpiration

392 per unit of leaf area did not differ much among water treatments and soil types in 2017 (Figure S8). The

393 opposite was the case for the transpiration rate per unit of root length. The observed root length at

394 different soil depths (Figure 2) and total root length for two plots in the stony soil was much smaller than

395 in the silty soil (Figure 3). Therefore, transpiration per unit of root length in the stony soils (F1P2 & F1P3)

396   was almost 3 times higher than transpiration in the silty soil. For the same soil, transpiration per unit root

397   length of the irrigated treatment was slightly larger than in the rainfed plot.

398   The differences in sap flow per plant between water treatments and soil types were more pronounced in

399   2018 (Figure S9). The highest transpiration rate was observed in the irrigated plots (F1P3 & F2P3), followed

400   by the rainfed plot of the silty soil (F2P2) and it was lowest in the rainfed plot of the stony soil (F1P2).

401   These observations were in line with the differences in biomass and leaf area index between the

402   treatments (Figure S3b & S3d) and plant size (Figure S6b-c-d). In 2018, severe leaf rolling was observed in

403   the rainfed plot (F1P2) from the beginning of June until the end of the growing period in 2018 (Figure S3d).

404   Similar to 2017, transpiration per unit of root length was much higher in the stony plots as compared to

405   silty plots. Also, for the silty soil, transpiration per unit of root length of the irrigated plot (F2P3) was higher

406   than in the rainfed plot (F2P2).

407   Higher cumulative transpiration in the irrigated plots did not result in higher transpiration use efficiency

408   (TUE) in both soil types (Figure 10). For instance, TUE were 16.87 g mm^{-1} and 15.59 g mm^{-1} for F1P2 and

409   F2P2, respectively, while they were 15.47 and 14.79 g mm^{-1} for F1P3 and F2P3, respectively, in 2017 (Figure

410   10A). For the same soil, the rainfed plot showed slightly higher TUE than the irrigated plot. When

411   comparing the TUE of maize of the two soil types for the same water treatment, TUE at the stony soil was

412   almost the same in silty soil. The TUE was not much different among treatments and soil types in 2018.

413   Overall, TUE in 2017 was higher as compared to 2018 (Fig. 10b).

414   [Insert Figure 10 here]

415   **4. Discussions**

416   **4.1. Effects of soil types, water application, and climatic condition on root growth**

417   Our root observations showed that soil type affected root growth more than water treatment (Figure 2).

418   Root growth was strongly inhibited by the stony soil where much lower root length was observed than in

419   the silty soil, especially in the deeper soil layers. This was consistent with the findings reported in

420   (Morandage et al., 2021) where a linear increase of stone content resulted in a linear decrease of rooting

421   depth across all stone contents and developmental stages. Also, both simulations and observations

422   indicated that rooting depth was increased due to the presence of cracks in the lower minirhizontron

423   facility (Morandage et al., 2021) which could explain the high root length between 40 and 120 cm soil

424   depths which was observed in the silty soil in both years.

425   In terms of the ratios of root length to shoot biomass, Ordóñez et al., (2020) has reported much larger

426   figures of for instance 880 cm g^{-1} in different locations and under different N application rates in maize

427   growing in the Midwest of US. Jorda et al., (2022) reported a wide range of ratios of root length to shoot

428   biomass from 200 to 1000 cm g^{-1} around flowering time of maize depending on the wild type and root hair

429   mutant genotypes growing on either loamy or sandy soils. More roots and higher ratios of root length to

430   shoot biomass were found in the sand than in the loam in both wild type and root hair mutant genotypes

431   (Jorda et al., 2022; Vetterlein et al., 2022). Cai et al., (2018) observed much larger ratios of root length to

432   shoot biomass in drought stressed plots than in irrigated plot in both soil types in winter wheat which

433   indicated the alternation of sink: source relationships to cope with water stress. This study emphasized

434   that more assimilates are used to promote root growth and extract more water under drought stress.

435   However, this was not the case for the stony soil in our work where the drought stress was more

436   pronounced, especially in 2018. A drop of soil water potential (Figure S2b), thus effective soil water

437   potential (Figure 6a) was substantial from 10th July 2018 toward the harvest in the rainfed plot in the silty

438   soil (F2P2) which was consistent with the reduction of leaf water potential (Fig. 6b), leaf area (Figure S3c),

439   total dry matter (Figure S3d), and crop height (Figure S6b) as compared the irrigated plot (F2P3). This

440   indicates a mild water stress in 2018 in the rainfed plots on the silty soil. The larger ratios of root length to

441   shoot biomass in this F2P2 plot in 2018 as compared to F2P3 could be explained by the change of source:

442   sink relations where more assimilates were devoted to root growth, even at a later growth stage.

443   Moreover, the low stone content and soil cracks (Morandage et al., 2021) might favor root growth in the

444   deeper soil layers which are close to the shallow soil water table in the rhizotrone facility with silty soil

445   (Vanderborght et al., 2010). In conclusion, both soil texture and water conditions influenced the root

446   growth, however, effects of the former on root length was more pronounced than the latter.

447   In the stony soil, which has a considerably smaller water holding capacity than the silty soil, root length

448   was considerably smaller than in the silty soil. Nevertheless, water uptake per unit root length was much

449   larger than in the fine soil. This also means that the hydraulic conductance per unit root length must have

450   been much larger in the stony soil than in the fine soil. Cai et al., (2018) observed a similar effect for winter

451   wheat but they found much smaller differences in the root length normalized root conductance. The

452   higher root length normalized root conductance means that the anatomy of the root tissues must have

453   been influenced by the soil texture and compensated the considerably smaller root length in the stony

454   soil. Looking at the effect of water treatments in the silt soil, the non-irrigated plot had more roots than

455   the irrigated one and both had more roots in the year with high VPD. But the soil-root conductance was

456   higher in the irrigated plot than in the rainfed plot. This means that in the irrigated plot, the soil-root

457   conductance per unit root length was higher than in the rainfed plot. This could either be due to wetter

458   soil conditions and higher soil conductance or it could be due to a larger conductance of the root tissues.

459   Especially in 2017 when the silty soil was wetter, the slightly larger soil-root conductance in the irrigated

460   plot is most likely the result of larger root tissue conductance in the irrigated plot. Thus, how root

461   architecture (here represented simply by the total root length) and root tissue conductivities 'respond' to

462   drought stress might be opposite depending on the comparisons that are made. When the stony soil and

463   silt soil are compared, the higher 'stress' due to lower water availability in the stony soil resulted in less

464   roots with a higher root tissue conductance in the soil with more stress. When comparing the rainfed with

465   the irrigated plot in the silty soil, the higher stress in the rainfed soil resulted in more roots with a lower

466   root tissue conductance in the treatment with more stress. This indicates that the response to water stress

467   can be different depending on soil conditions or water treatments.

4.2. Effects of soil types, water application, and climatic condition on stomatal conductance,

photosynthesis, transpiration, leaf water potential, and plant hydraulic conductance

4.2.1. Leaf water potential and stomatal conductance as affected by soil water conditions

471   In the previous work, Koehler et al., (2022) reported that maize stomata closed at lower negative leaf

472   water potentials in sand than in loam growing under controlled environment. Cai et al., (2022b)

473   investigated transpiration response of pot-grown maize in two contrasting soil textures (sand and loam)

474   and exposed to two consecutive VPD levels (1.8 and 2.8 kPa). Transpiration rate decreased at less negative

475   soil matric potential in sand than in loam at both VPD levels. In sand, high VPD generated a steeper drop

476   in stomatal conductance with decreasing leaf water potential which indicated that the transpiration and

477   stomatal responses depend on soil hydraulics. In our study, stomata closed earlier and at more negative

478   soil and leaf water potentials in the stony soil than in the silty soil (see Fig. 4 & 7 and Figure S4 & S5). The

479   lower soil water holding capacity of the stony soil compared to the silty soil resulted in lower soil water

480   potential and smaller total plant hydraulic conductance which in turn led to earlier stomatal closure and

481   to more negative soil water potential in the stony soil.

482   Stomatal control is an early and effective response to water stress to prevent the plant from water loss

483   and dehydration. Maize is considered as an isohydric plant which closes its stomata to maintain leaf water

484   potential above critical levels (Tardieu and Simonneau, 1998). Our results showed that minimum leaf

485   water potential varied among treatments (-1.5 MPa for F1P3, F2P2, and F2P3 and up to -2 MPa for F1P2

486   in 2017, while in 2018 minimum values were -2 MPa for F2P3, F2P2, and F2P3 and -2.7 MPa for F1P2) (Fig.

487   5, Fig. 6, and Fig. 7). In conclusion, our results confirmed that the minimum ψ_{leaf} not only depended on

488   genotypic differences but also was influenced by soil types, soil hydraulic conductance, and atmospheric

489   demand.

4.2.2. Hydraulic conductance components as affected by soil water conditions

491   Estimates of hydraulic components in soil-plant-atmosphere continuum are important not only to

492   understand its underlying relationship to other crop characteristics (stomatal conductance, transpiration,

493   and photosynthesis) but also to provide modeling parameters in process-based soil-root-shoot models

494   (Nguyen et al., 2020; Sulis et al., 2019; Nguyen et al., 2022b). Measurement of the components of hydraulic

495   conductance are challenging under field conditions because it requires the estimation of transpiration and

496   root to leaf water potential gradients. To our knowledge, our results were unique with regard to the

497   dynamics of K_{soil_plant} for field-grown maize on two soil types and under contrasting water, and climatic

498   conditions. Our seasonal K_{soil_plant} ranged from 0.12 mm h^{-1} MPa^{-1} to 0.9 mm h^{-1} MPa^{-1} (Fig. 6 & Fig. 7; Fig.

499   8, and Figure S7). Root system hydraulic conductance ranged from 0.26 to 1.47 mm h^{-1} MPa^{-1} (Figure 9).

500   Note that the unit of K_{soil_plant} as mm h^{-1} MPa^{-1} could be equivalent to the unit of 10^{-5} h^{-1} if one assumes

501   1MPa is approximately 10^5 mm in terms of pressure head. Cai et al., (2018) reported root hydraulic

502   conductance in winter wheat from 0.05 to 0.5 mm h^{-1} MPa^{-1} in two similar soil types. Nguyen et al., (2020)

503   also reported K_{soil_plant} in winter wheat from 0.0625 to 0.461 mm h^{-1} MPa^{-1}. Meunier et al., (2018) focused

504   on estimating the root system hydraulic conductance of maize in a container experiment where the range

505   of K_{soil_plant} was much larger from 0.37 to 36 mm h^{-1} MPa^{-1} for the plant density of 10 plant m^{-2}. Jorda et al.,

506   (2022) estimated root system hydraulic conductance of 0.5 to 1.5 10^{-3} d^{-1} which would be roughly between

507   2 to 6 mm h^{-1} MPa^{-1}. In our work, except the F2P2 in 2018, the stem hydraulic conductance was 10% to

508   60% higher than root system hydraulic conductance. Gallardo et al., (1996) reported that stem hydraulic

509   conductance of wheat was lower than root system conductance at around 71 to 91 days after sowing

510   (DAS), but they were similar at 102 DAS. In lupine, stem hydraulic conductance was two times higher than

511   root system conductance regardless of measured days. The larger root length in wheat than lupine did not

512 necessarily result in higher root conductance in wheat. Together with this study, our study emphasizes the

513 values of stem hydraulic conductance compared to the root hydraulic conductance in maintaining water

514 potential gradient from shaded leaf or plant color to the sunlit leaf.

515 Our results showed clear differences in K_{soil_plant} among treatments where much lower K_{soil_plant} was

516 observed in the F1P2 as compared to F2P2 (see Figure 8 for 2018; Figure 6 and 7 and Figure S7 for both

517 years). This indicated the soil texture dependence for whole plant hydraulic conductance. Maize plants

518 with the shorter root system (i.e. rainfed plot in the stony soil in 2018) (Fig. 3) had lower plant hydraulic

519 conductance. Our results indicated that there was an impact of soil hydraulic conditions on K_{soil_plant} via the

520 reduction of root system hydraulic conductance. Our analysis for three consecutive measurement days in

521 2018 (Fig 8) showed that in the silty soil, K_{soil_plant} decrease when soil water potentials are becoming more

522 negative. For instance, in the silty soil in 2018 when the soil water potentials were considerably lower in

523 the rainfed than in the irrigated plot (e.g. after 10th July), K_{soil_plant} was lower in the rainfed than in the

524 irrigated plot. In the stony soil, the K_{soil_plant} and leaf water potentials seems to decrease more considerably

525 (compared to the silty soil) when the soil water potentials become more negative. In other words, K_{soil_plant}

526 increased considerably when the soil water potentials in the stony soil increased. In our work, K_{soil_plant}

527 increased slowly after irrigation mainly for the severe water stress plot (see F1P2 on 19 July in Fig 7d and

528 8c). This implied that added soil water by irrigation took some time for recovery the soil-root contact within

529 the rhizophere.

530 **4.2.3. Relationships of stomatal conductance, transpiration, photosynthesis with plant hydraulic**

531 **variables**

532 The transpiration rate and K_{soil_plant} (slope of linear regression lines in Fig. 8a and b) were very low in the

533 rainfed plot under the stony soil (F1P2) which was associated with the large $\psi_{difference}$ (Fig. 8a & b) and the

534 lower stomatal conductance as compared to other plots (Fig. 7c). The K_{soil_plant} slightly increased after

535 irrigation (18 July - DOY 199 in Fig. 8b) corresponding with the smaller $\psi_{difference}$ (Fig. 8b) and an increase in

536   stomatal conductance (Fig. 7c). Seasonal K_{soil_plant} was low in the rainfed plot under stony soil (F1P2) with

537   the larger $\psi_{difference}$ (Figure S7). In addition, our study showed that the midday stomatal conductance,

538   photosynthesis, and transpiration were significantly correlated only with midday K_{soil_plant} in the rainfed

539   plot on the stony soil (F1P2) in 2018 where high VPD and temperature occurred (Table S1, Figure S10, and

540   S11). Maize plants had lower plant hydraulic conductance and more negative soil water potential in the

541   rainfed plot in stony soil that and they exhibited earlier stomatal closure as compared to the same plot in

542   the silty soil. This was in line with a study from Abdalla et al., (2022) which suggested that during soil

543   drying, stomatal regulation of tomato is controlled by root and soil hydraulic conductance. Recent work

544   from Müllers et al., (2022) on faba bean and maize suggested that differences in the stomatal sensitivity

545   among plant species can be partly explained by the sensitivity of soil-plant hydraulic conductance to soil

546   drying. The loss of conductance has immediate consequences for leaf water potential and the associated

547   stomatal regulation. Cai et al., (2022b) also showed that the decrease in sunlit leaf stomatal conductance

548   was well correlated with the drop in soil-plant hydraulic conductance, which was significantly affected by

549   soil texture. This was confirmed in our work where the stony soil strongly impacted on root growth,

550   modulated $K_{soil\_plant,}$ and consequently influenced the leaf stomatal conductance, photosynthesis, and

551   transpiration.

552   **4.3. Relative contribution of water control by leaves and roots on transpiration and transpiration use**

553   **efficiency**

554   Responses of crops via stomatal control to reduce water loss at leaf scale while maintaining leaf

555   photosynthesis and water use efficiency were reported earlier (Nguyen et al., 2022a; Vitale et al., 2007).

556   In addition to that, in the maize experiments in 2017 and 2018 leaf rolling was observed in both rainfed

557   plots on the stony and the silty soil in the second week of June 2017 and from the beginning of June until

558   the end of the growing period in 2018. This indicates another dehydration avoidance mechanism resulting

559   from morphological adjustments which is an effective strategy to leaf senescence (Aparicio-Tejo and

560   Boyer, 1983; Richards et al., 2002). Stomatal closure resulted in more reduction of transpiration and

561   assimilation in the rainfed plots than irrigated plots with the same soil type (Fig. 4, Figure S4 & S5, Fig. 5,

562   and Figure S9a). There was reduction of shoot biomass (also stem size and leaf size adjustments) in F1P2

563   as compared to other plots. However, the TUE was not smaller in this plot than the remaining plots. These

564   observations confirm that plant size adjustments through reduction of height, leaf width and length are

565   efficient responses to reduce water loss at canopy scale in addition to stomatal control at the leaf level.

566   Relative contribution of leaf area to transpiration has been highlighted in wheat where reduction of tiller

567   number resulted in significantly lower LAI, thus lower canopy transpiration (Cai et al., 2018; Trillo and

568   Fernández, 2005; Nguyen et al., 2022a). However, root system conductance per unit of leaf area and per

569   unit root mass were strongly reduced and eventually more than reduction of leaf area under water stress

570   (Trillo and Fernández, 2005). In our work, expressing the transpiration per unit of root length on the one

571   hand allowed to analyze the role of total root length to water uptake. However, on the other hand, the

572   lower total root length did not necessarily result in a lower root water uptake and vice versa. For instance,

573   the rainfed plot of the treatment F2P2 had the larger total root length which could postpone the effect of

574   soil water limitations in drying soils due to greater ability to extract water from subsoils. Therefore,

575   transpiration was very similar between F2P2 and F2P3. Despite of the much lower total root length in the

576   stony soil, K_{soil_plant} in the irrigated plot (F1P3) was not much lower than in the same water treatment in

577   the silty soil (F2P3, Fig. 6d, 7d, Fig. 8, and Figure S7). This could be explained by the fact that the K_{soil_plant}

578   variability was not only depended on root architecture (here the root length and distribution) but also

579   depended on the variability of root segment hydraulic properties which has also been illustrated and

580   discussed in Zwieniecki et al. (2002), Frensch and Steudle (1989), Meunier et al. (2018), Couvreur et al.

581   (2014), and Ahmed et al. (2018). Moreover, the contribution of shoot hydraulic conductance could be large

582   in plants (Gallardo et al., 1996; Trillo and Fernández, 2005; Sunita et al., 2014) which also confirmed in our

583   work. In our work, K_{soil_plant} comprised root and shoot conductance which are directly influenced by soil

584 hydraulics. Our estimates of K_{soil_plant} varied with transpiration and gradients of $\psi_{sunlitleaf}$ and ψ_{soil_effec}. Thus,

585 any change of soil hydraulic conductance will change the root to shoot water potential. Consequently, it

586 will affect the gradients between shoot and root rhizosphere (Carminati and Javaux, 2020). Thus, our study

587 is revealing the importance of both soil texture characteristics and root phenotypic traits (here root length)

588 in regulating plant transpiration (Cai et al., 2022a). Despite of lower root length in the stony irrigated plot,

589 transpiration rate was not much lower than in the silty irrigated plot in our work. This could be related to

590 another property of the root such as root segment conductance or other root traits (e.g. root hair). Further

591 investigation with extensive measurements of roots including axial and radial root conductance at field

592 scale will be required to better explain the observed results. Other traits like root hair density (Cai et al.,

593 2022a) or higher root length density (Vadez, 2014) could contribute to the soil to root water potential and

594 root-zone hydraulic conductance where dense root hairs are delaying soil water deficit in drying soils.

595 However, contrasting results have shown that root hairs did not have an effect on root water uptake (see

596 Jorda et al. 2022). The role of root hairs could not be analyzed in our work which was based on the root

597 data from minirhizotron images.

598 This study investigated soil-water-plant relations, more specifically the interactions of the root and shoot

599 growth processes and water fluxes under variations of soil water status and atmospheric demands. To the

600 best of our knowledge, the comprehensive data collected from soil to root, plant, and atmosphere under

601 field conditions in this work was unique. However, we acknowledged the lack of treatment replicates

602 which was due to the complex and expensive construction of the rhizotrone facilities. We also

603 acknowledged the small size of plots that did not allow the extensive destructive sampling (i.e. leaf area,

604 biomass, or determination of leaf water potential etc.). Each rhizotrone site originally contained the

605 irrigated, rainfed, and rain-out sheltered plots (Nguyen et al., 2022a; Cai et al., 2016). The overall aim of

606 the experiments was to investigate the root and shoot responses and gas fluxes (CO_2 and H_2O) of wheat

607 and maize to the variations of soil water and soil hydraulics. Note that the studies did not intend to

608   investigate the impacts of similar irrigation strategies on plant water status among seasons (i.e. in 2017

609   and 2018) because the irrigation practices were less common in the regions. The collapse of manual rain-

610   out shelters due to strong wind after the 2016 growing season resulted in only two water treatments

611   (rainfed and irrigated). Based on experiences from the previous seasons (wheat), we argued that such

612   combinations of two water treatments and two soil types, to some extent, could still create a wide range

613   of soil water conditions for the maize trial. For instance, the "rainfed" treatment at the stony soil in the

614   upper rhizotrone (F1P2) could lead to severe water stress compared to other treatments, especially in the

615   summertime when the atmospheric evaporative demand is high. In fact, mild water stress was observed

616   at the F1P2 around mid -June in 2017. In 2018, the sites were slightly modified to induce more severe

617   water stress (Nguyen et al., 2022a). One rainfed plot with the stony soil had late sowing while one rainfed

618   plot with the silty soil had the higher sowing density (data not shown in the study). Unprecedented

619   weather (extremely hot and dry) in 2018 resulted in severe drought stress at the rainfed plots with the

620   stony soil. To compare the effects of soil types and water treatments on crop, we presented here only data

621   from two plots (rainfed and irrigated) for two soil types. In spite of the experimental limitations, the

622   relative differences among the treatments, soil types, and seasons as well as measured dates were clearly

623   illustrated which ultimately supported the overall aim of our study.

624   The simultaneous measurements of atmospheric conditions, leaf water potential, and transpiration rates,

625   coupled with measurements of root, stem and whole soil-plant hydraulic conductance, root architecture

626   (root length), and soil water potential distribution illustrated the complex responses of the shoot and root

627   growth and hydraulic conductance vulnerability to soil water availability. The different responses of crop

628   processes to soil hydraulics and climatic conditions suggest further field investigations for other soil types,

629   growing seasons, and water regimes. Future studies considering the effects of progressive soil drying or

630   irrigation strategies on plant water status and crop growth at field conditions will be necessary. This is very

631   relevant for those crop-growing regions that require irrigation. Our results show that the leaf water

632   potential threshold can vary within the same genotype depending on soil types, climatic conditions, and

633   water management. Large variability of minimum leaf water potential has been reported for maize

634   genotypes under greenhouse conditions (Welcker et al., 2011). Field studies are required concerning the

635   stomatal functions, water relations, hydraulic vulnerability traits, and root: shoot responses, especially of

636   different maize cultivars in responding to drought stress. This will suggest implications for selecting

637   agronomic cultivars and traits under changing climates. Results from this study show that soil-crop models

638   should focus not only on simulating stomatal regulations to capture the response to drought stress, but

639   also require adequate representations of root and leaf growth and adjustments. The soil hydraulics

640   strongly influenced soil water availability and crop growths. Regional applications of soil-crop models for

641   simulating gas fluxes and crop growth processes and for estimating irrigation amounts must account for

642   the environmental heterogeneity within the spatial simulation unit whereas the soil heterogeneity is the

643   key variable.

644   **5. Conclusion**

645   We presented plant hydraulic characteristics and crop growth from root to shoot of maize under field-

646   grown conditions with two soil types (silty and stony), each soil with two water regimes (irrigated and

647   rainfed) for two growing seasons (2017, 2018). Our results confirmed that root length and ratios of root

648   length to shoot biomass were modulated by soil types and water treatment but less by seasonal

649   evaporative demand. Increase ratio of root length to shoot biomass was an important response of maize

650   that allows plants to extract more water under drought stress that occurred rather in the silty soil but less

651   in the stony soil due to the higher content of stony material.

652   Another conclusion is that stomatal regulation maintains leaf water potential at certain thresholds which

653   depends on soil types, soil water availability, and seasonal atmospheric demand. The stomata conductance

654   was smaller and decreased at more negative leaf water potentials in stony soil than in silty soil. The leaf

655   water potentials are affected by the soil-plant hydraulic conductance. In addition to stomatal regulation,

656 leaf growth and plant size adjustments are important to regulate the transpiration and water use efficiency

657 in the same year.

658 The lowest soil-plant hydraulic conductance was observed in the stony soil with severe drought stress as

659 compared to silty soil while its variation depends also on the soil water variation (before and after

660 irrigation). Root system and soil-plant hydraulic conductance depended strongly on soil hydraulic

661 properties. The 'response' to stress can be completely opposite depending on conditions or treatments

662 that lead to the differences in stress that are compared. Therefore, it cannot be the 'stress' alone that

663 defines how a plant will react and adapt its root system. Modelling the impact of stress and the feedback

664 between drought stress and plant development is likely controlled by other properties or parameters that

665 change with changing soil water availability and atmospheric water demand then the plant stress level.

666 **Acknowledgements**

667 This work has partially been funded by Federal Ministry of Education and Research (BMBF) through

668 European SUSCAP project – 031B0170B and COINS project - 01LL2204C and the Deutsche

669 Forschungsgemeinschaft (DFG, German Research Foundation) under Germany's Excellence Strategy – EXC

670 2070 – 390732324. We acknowledge the support by the SFB/TR32 "Pattern in Soil–Vegetation–

671 Atmosphere Systems: Monitoring, Modelling, and Data Assimilation" funded by the Deutsche

672 Forschungsgemeinschaft (DFG). Thuy Nguyen and Thomas Gaiser also thank the DETECT – CRC 1502

673 research program which is funded by DFG. We thank Dr. Matthias Langensiepen for his supports and

674 technical help in the TR32 project. We would like to thank all the student assistants and technicians for

675 their considerable efforts to collect the data in the field and the laboratories.

676 **Reference**

677 Abdalla, M., M.A. Ahmed, G. Cai, F. Wankmüller, N. Schwartz, et al. 2022. Stomatal closure during water
678   deficit is controlled by below-ground hydraulics. Ann. Bot. 129(2): 161–170. doi:
679   10.1093/aob/mcab141.

680 Abdalla, M., A. Carminati, G. Cai, M. Javaux, and M.A. Ahmed. 2021. Stomatal closure of tomato under
681   drought is driven by an increase in soil-root hydraulic resistance. Plant. Cell Environ. 44(2): 425–
682   431. doi: 10.1111/pce.13939.

683 Ahmed, M.A., M. Zarebanadkouki, F. Meunier, M. Javaux, A. Kaestner, et al. 2018. Root type matters:
684   Measurement of water uptake by seminal, crown, and lateral roots in maize. J. Exp. Bot. 69(5): 1199–
685   1206. doi: 10.1093/jxb/erx439.

686 Allen, R.G., Pereira, L.S., Raes, D., Smith, M., 1998. FAO Irrigation and Drainage Paper – Crop
687   Evapotranspiration. FAO, Italy.

688 Aparicio-Tejo, P., and J.S. Boyer. 1983. Significance of Accelerated Leaf Senescence at Low Water Potentials
689   for Water Loss and Grain Yield in Maize1. Crop Sci. 23(6): cropsci1983.0011183X002300060040x. doi:
690   https://doi.org/10.2135/cropsci1983.0011183X002300060040x.

691 Bauer, F.M., L. Lärm, S. Morandage, G. Lobet, J. Vanderborght, et al. 2021. Combining deep learning and
692   automated feature extraction to analyze minirhizotron images: development and validation of a new
693   pipeline.   bioRxiv   (1):   2021.12.01.470811.
694   https://www.biorxiv.org/content/10.1101/2021.12.01.470811v1%0Ahttps://www.biorxiv.org/cont
695   ent/10.1101/2021.12.01.470811v1.abstract.

696 Bornemann*, L., M. Herbst, G. Welp, H. Vereecken, and W. Amelung. 2011. Rock Fragments Control Size
697   and Saturation of Organic Carbon Pools in Agricultural Topsoil. Soil Sci. Soc. Am. J. 75(5): 1898. doi:
698   10.2136/sssaj2010.0454.

699 Bourbia, I., C. Pritzkow, and T.J. Brodribb. 2021. Herb and conifer roots show similar high sensitivity to
700   water deficit. Plant Physiol. 186(4): 1908–1918. doi: 10.1093/plphys/kiab207.

701 Cai, G., M.A. Ahmed, M. Abdalla, and A. Carminati. 2022a. Root hydraulic phenotypes impacting water
702   uptake in drying soils. Plant Cell Environ. 45(3): 650–663. doi: 10.1111/pce.14259.

703 Cai, G., M. König, A. Carminati, M. Abdalla, M. Javaux, et al. 2022b. Transpiration response to soil drying
704   and vapor pressure deficit is soil texture specific. Plant Soil (0123456789). doi: 10.1007/s11104-022-
705   05818-2.

706 Cai, G., J. Vanderborght, V. Couvreur, C.M. Mboh, and H. Vereecken. 2017a. Parameterization of Root
707   Water Uptake Models Considering Dynamic Root Distributions and Water Uptake Compensation.
708   Vadose Zo. J. 0(0): 0. doi: 10.2136/vzj2016.12.0125.

709 Cai, G., J. Vanderborght, A. Klotzsche, J. van der Kruk, J. Neumann, et al. 2016. Construction of
710   Minirhizotron Facilities for Investigating Root ZoneProcesses. Vadose Zo. J. 15(9): 0. doi:
711   10.2136/vzj2016.05.0043.

712 Cai, G., J. Vanderborght, M. Langensiepen, A. Schnepf, H. Hüging, et al. 2018. Root growth, water uptake,
713   and sap flow of winter wheat in response to different soil water conditions. Hydrol. Earth Syst. Sci.
714   22(4): 2449–2470. doi: 10.5194/hess-22-2449-2018.

715 Cai, Q., Y. Zhang, Z. Sun, J. Zheng, W. Bai, et al. 2017b. Morphological plasticity of root growth under mild
716   water stress increases water use efficiency without reducing yield in maize. Biogeosciences 14(16):
717   3851–3858. doi: 10.5194/bg-14-3851-2017.

718 Carminati, A., and M. Javaux. 2020. Soil Rather Than Xylem Vulnerability Controls Stomatal Response to
719   Drought. Trends Plant Sci. 25(9): 868–880. doi: 10.1016/j.tplants.2020.04.003.

720 Carminati, A., M. Zarebanadkouki, E. Kroener, M.A. Ahmed, and M. Holz. 2016. Biophysical rhizosphere
721   processes affecting root water uptake. Ann. Bot. 118(4): 561–571. doi: 10.1093/aob/mcw113.

722 Choudhary, S., and T.R. Sinclair. 2014. Hydraulic conductance differences among sorghum genotypes to
723   explain variation in restricted transpiration rates. Funct. Plant Biol. 41(3): 270–275. doi:
724   10.1071/FP13246.

725 Cochard, H. 2002. Xylem embolism and drought-induced stomatal closure in maize. Planta 215(3): 466–
726   471. doi: 10.1007/s00425-002-0766-9.

727 Comas, L.H., S.R. Becker, V.M. V. Cruz, P.F. Byrne, and D.A. Dierig. 2013. Root traits contributing to plant
728   productivity under drought. Front. Plant Sci. 4(NOV): 1–16. doi: 10.3389/fpls.2013.00442.

729 Coupel-Ledru, A., É. Lebon, A. Christophe, A. Doligez, L. Cabrera-Bosquet, et al. 2014. Genetic variation in
730   a grapevine progeny (Vitis vinifera L. cvs GrenachexSyrah) reveals inconsistencies between
731   maintenance of daytime leaf water potential and response of transpiration rate under drought. J.
732   Exp. Bot. 65(21): 6205–6218. doi: 10.1093/jxb/eru228.

733 Couvreur, V., J. Vanderborght, X. Draye, and M. Javaux. 2014. Dynamic aspects of soil water availability for
734   isohydric plants: Focus on root hydraulic resistances. water Resour. Res. 50: 8891–8906. doi:
735   10.1002/2014WR015608.Received.

736 Couvreur, V., J. Vanderborght, and M. Javaux. 2012. A simple three-dimensional macroscopic root water
737   uptake model based on the hydraulic architecture approach. Hydrol. Earth Syst. Sci. 16: 2957–2971.
738   doi: 10.5194/hess-16-2957-2012.

739 Daryanto, S., L. Wang, and P. Jacinthe. 2016. Global Synthesis of Drought Effects on Maize and Wheat
740   Production. PLoS One 11(5): 1–15. doi: 10.1371/journal.pone.0156362.

741 Draye, X., Y. Kim, G. Lobet, and M. Javaux. 2010. Model-assisted integration of physiological and
742   environmental constraints affecting the dynamic and spatial patterns of root water uptake from
743   soils. J. Exp. Bot. 61(8): 2145–2155. doi: 10.1093/jxb/erq077.

744 Domec, J., and D.M. Johnson. 2012. Does homeostasis or disturbance of homeostasis in minimum leaf
745   water potential explain the isohydric versus anisohydric behavior of Vitis vinifera L . cultivars ? Tree
746   32: 245–248. doi: 10.1093/treephys/tps013.

747 Domec, J., and M.L. Pruyn. 2008. Bole girdling affects metabolic properties and root , trunk and branch
748   hydraulics of young ponderosa pine trees. Tree Physiol. (28): 1493–1504.

749 Dynamax. 2007. Dynagage Sap Flow Sensor User Manual. 1–107. Last access on March 5th 2015.

750 Effendi, R., S.B. Priyanto, M. Aqil, and M. Azrai. 2019. Drought adaptation level of maize genotypes based
751   on leaf rolling, temperature, relative moisture content, and grain yield parameters. IOP Conf. Ser.
752   Earth Environ. Sci. 270(1). doi: 10.1088/1755-1315/270/1/012016.

753 Fang, J., and Y. Su. 2019. Effects of Soils and Irrigation Volume on Maize Yield, Irrigation Water Productivity,
754   and Nitrogen Uptake. Sci. Rep. 9(1): 1–11. doi: 10.1038/s41598-019-41447-z.

755 Frensch, J., and E. Steudle. 1989. Axial and Radial Hydraulic Resistance to Roots of Maize (Zea mays L.).
756   Plant Physiol. 91: 719–726.

757 Gallardo, M., J. Eastham, P.J. Gregory, and N.C. Turner. 1996. A comparison of plant hydraulic
758   conductances in wheat and lupins. J. Exp. Bot. 47(295): 233–239. doi: 10.1093/jxb/47.2.233.

759 Hochberg, U., F.E. Rockwell, N.M. Holbrook, and H. Cochard. 2018. Iso/Anisohydry: A Plant–Environment
760   Interaction Rather Than a Simple Hydraulic Trait. Trends Plant Sci. 23(2): 112–120. doi:
761   10.1016/j.tplants.2017.11.002.

762 Hopmans, J.W., and K.L. Bristow. 2002. Current Capabilities and Future Needs of Root Water and
763   Nutrient Uptake Modeling. In: Sparks, D.L.B.T.-A. in A., editor, Advances in Agronomy. Academic
764   Press. p. 103–183

765 Hubbard, R.M., M.G. Ryan, V. Stiller, and J.S. Sperry. 2001. Stomatal conductance and photosynthesis vary
766   linearly with plant hydraulic conductance in ponderosa pine. Plant, Cell Environ. 24(1): 113–121. doi:
767   10.1046/j.1365-3040.2001.00660.x.

768 IPCC. 2022. Impacts, Adaptation, and Vulnerability. Working Group II Contribution to the IPCC Sixth
769   Assessment Report of the Intergovernmental Panel on Climate Change.

770 Jorda, H., M.A. Ahmed, M. Javaux, A. Carminati, P. Duddek, et al. 2022. Field scale plant water relation of
771   maize (Zea mays) under drought – impact of root hairs and soil texture. Plant Soil 478(1–2): 59–84.
772   doi: 10.1007/s11104-022-05685-x.

773 Klein, T. 2014. The variability of stomatal sensitivity to leaf water potential across tree species indicates a
774   continuum between isohydric and anisohydric behaviours. Funct. Ecol.: 1313–1320. doi:
775   10.1111/1365-2435.12289.

776 Koehler, T., D.S. Moser, Á. Botezatu, T. Murugesan, S. Kaliamoorthy, et al. 2022. Going underground: soil
777   hydraulic properties impacting maize responsiveness to water deficit. Plant Soil 478(1–2): 43–58. doi:
778   10.1007/s11104-022-05656-2.

779 Lärm, L., F.M. Bauer, N. Hermes, J. van der Kruk, H. Vereecken, et al. 2023. Multi-year belowground data
780   of minirhizotron facilities in Selhausen. Sci. Data 10(1): 1–15. doi: 10.1038/s41597-023-02570-9.

781 Li, X., T.R. Sinclair, and L. Bagherzadi. 2016. Hydraulic Conductivity Changes in Soybean Plant-Soil System
782   with Decreasing Soil Volumetric Water Content. J. Crop Improv. 30(6): 713–723. doi:
783   10.1080/15427528.2016.1231729.

784 Li, Y., J.S. Sperry, and M. Shao. 2009. Hydraulic conductance and vulnerability to cavitation in corn (Zea
785   mays L.) hybrids of differing drought resistance. Environ. Exp. Bot. 66(2): 341–346. doi:
786   10.1016/j.envexpbot.2009.02.001.

787 Marin, M., D.S. Feeney, L.K. Brown, M. Naveed, S. Ruiz, et al. 2021. Significance of root hairs for plant
788   performance under contrasting field conditions and water deficit. Ann. Bot. 128(1): 1–16. doi:
789   10.1093/aob/mcaa181.

790 Meunier, F., A. Heymans, X. Draye, V. Couvreur, M. Javaux, et al. 2020. MARSHAL, a novel tool for virtual
791   phenotyping of maize root system hydraulic architectures. In Silico Plants 2(1): 1–15. doi:
792   10.1093/insilicoplants/diz012.

793 Meunier, F., M. Zarebanadkouki, M.A. Ahmed, A. Carminati, V. Couvreur, et al. 2018. Hydraulic
794   conductivity of soil-grown lupine and maize unbranched roots and maize root-shoot junctions. J.
795   Plant Physiol. 227(February): 31–44. doi: 10.1016/j.jplph.2017.12.019.

796 Morandage, S., J. Vanderborght, M. Zörner, G. Cai, D. Leitner, et al. 2021. Root architecture development
797   in stony soils. Vadose Zo. J. (April): 1–17. doi: 10.1002/vzj2.20133.

798 Müllers, Y., J.A. Postma, H. Poorter, and D. van Dusschoten. 2022. Stomatal conductance tracks soil-to-leaf

799   hydraulic conductance in faba bean and maize during soil drying. Plant Physiol. doi:
800   10.1093/plphys/kiac422.

801   Nguyen, T.H., M. Langensiepen, T. Gaiser, H. Webber, H. Ahrends, et al. 2022a. Responses of winter wheat
802   and maize to varying soil moisture: From leaf to canopy. Agric. For. Meteorol. 314(December 2021):
803   108803. doi: 10.1016/j.agrformet.2021.108803.

804   Nguyen, T.H., M. Langensiepen, H. Hueging, T. Gaiser, S.J. Seidel, et al. 2022b. Expansion and evaluation
805   of two coupled root–shoot models in simulating CO_2 and H_2O fluxes and growth of maize. Vadose
806   Zo. J. 21(3): 1–31. doi: 10.1002/vzj2.20181.

807   Nguyen, T.H., M. Langensiepen, J. Vanderborght, H. Hüging, C.M. Mboh, et al. 2020. Comparison of root
808   water uptake models in simulating CO_2 and H_2O fluxes and growth of wheat. Hydrol. Earth Syst. Sci.
809   (24): 4943–4969. doi: 10.5194/hess-24-4943-2020.

810   Nguyen, T.H, G. Lopez, S.J. Seidel, L. Lärm, F.M. Bauer, et al. 2024b. Multi-year aboveground data of
811   minirhizotron facilities in Selhausen. Sci. Data 11(1): 1–11. doi.org/10.1038/s41597-024-03535-2

812   Ordóñez, R.A., S. V. Archontoulis, R. Martinez-Feria, J.L. Hatfield, E.E. Wright, et al. 2020. Root to shoot
813   and carbon to nitrogen ratios of maize and soybean crops in the US Midwest. Eur. J. Agron. 120(June):
814   126130. doi: 10.1016/j.eja.2020.126130.

815   Passioura, J.B., 2006. The perils of pot experiments. Funct. Plant Biol. 33 (12), 1075–1079.
816   https://doi.org/10.1071/FP06223.

817   Ranawana SRWMCJK, Siddique KHM, Palta JA et al (2021) Stomata coordinate with plant hydraulics to
818   regulate transpiration response to vapour pressure defcit in wheat. Functional Plant Biol 48:839–850.
819   https://doi.org/10.1071/FP20392

820   Richards, R.A., G.J. Rebetzke, A.G. Condon, and A.F. van Herwaarden. 2002. Breeding Opportunities for
821   Increasing the Efficiency of Water Use and Crop Yield in Temperate Cereals. Crop Sci. 42(1): 111–
822   121. doi: 10.2135/cropsci2002.1110.

823   Rodriguez-Dominguez, C.M., and T.J. Brodribb. 2019. Declining root water transport drives stomatal
824   closure in olive under. New Phytol. 225: 126–134.

825   Sinclair, T.R., and M.M. Ludlow. 1986. Influence of soil water supply on the plant water balance of four
826   tropical grain legumes. Aust. J. Plant Physiol. 13: 329–341.

827   Scharwies, J.D., and J.R. Dinneny. 2019. Water transport, perception, and response in plants. J. Plant Res.
828   132(3): 311–324. doi: 10.1007/s10265-019-01089-8.

829   Schultz, H.R. 2003. Differences in hydraulic architecture account for near-isohydric and anisohydric
830   behaviour of two field-grown Vitis vinifera L. cultivars during drought. Plant, Cell Environ. 26(8):
831   1393–1405. doi: 10.1046/j.1365-3040.2003.01064.x.

832   Stadler, A., S. Rudolph, M. Kupisch, M. Langensiepen, J. van der Kruk, et al. 2015. Quantifying the effects
833   of soil variability on crop growth using apparent soil electrical conductivity measurements. Eur. J.
834   Agron. 64: 8–20. doi: 10.1016/j.eja.2014.12.004.

835   Sulis, M., V. Couvreur, J. Keune, G. Cai, I. Trebs, et al. 2019. Incorporating a root water uptake model based
836   on the hydraulic architecture approach in terrestrial systems simulations. Agric. For. Meteorol. 269–
837   270: 28–45. doi: https://doi.org/10.1016/j.agrformet.2019.01.034.

838   Sunita, C., T.R. Sinclair, C.D. Messina, and M. Cooper. 2014. Hydraulic conductance of maize hybrids

839   differing in transpiration response to vapor pressure deficit. Crop Sci. 54(3): 1147–1152. doi:
840   10.2135/cropsci2013.05.0303.

841   Tardieu, F., X. Draye, and M. Javaux. 2017. Root Water Uptake and Ideotypes of the Root System: Whole-
842   Plant Controls Matter. Vadose Zo. J. 16(9): 0. doi: 10.2136/vzj2017.05.0107.

843   Tardieu, F., and T. Simonneau. 1998. Variability among species of stomatal control under fluctuating soil
844   water status and evaporative demand: modelling isohydric and anisohydric behaviours. J. Exp. Bot.
845   49(March): 419–432. doi: 10.1093/jxb/49.Special_Issue.419.

846   Tardieu, F. 2016. Too many partners in root – shoot signals . Does hydraulics qualify as the only signal
847   that feeds back over time for reliable stomatal. New Phytol. 212: 802–804.

848   Trillo, N., and R.J. Fernández. 2005. Wheat plant hydraulic properties under prolonged experimental
849   drought: Stronger decline in root-system conductance than in leaf area. Plant Soil 277(1–2): 277–
850   284. doi: 10.1007/s11104-005-7493-5.

851   Tsuda, M., and M.T. Tyree. 1997. Whole-plant hydraulic resistance and vulnerability segmentation in
852   Acer saccharinum. Tree Physiol. (17): 351–357.

853   Turner, N.C., E.D. Schulze, and T. Gollan. 1984. The responses of stomata and leaf gas exchange to vapour
854   pressure deficits and soil water content - I. Species comparisons at high soil water contents.
855   Oecologia 63(3): 338–342. doi: 10.1007/BF00390662.

856   Tyree, M.T., E.L. Fiscus, S.D. Wullschleger, and M.A. Dixon. 1986. Detection of Xylem Cavitation in Corn
857   under Field Conditions. Plant Physiol. 82(2): 597–599. doi: 10.1104/pp.82.2.597.

858   Vadez, V. 2014. Root hydraulics : The forgotten side of roots in drought adaptation. F. Crop. Res. 165: 15–
859   24.

860   Vadez, V., S. Choudhary, J. Kholová, C.T. Hash, R. Srivastava, et al. 2021. Transpiration efficiency: Insights
861   from comparisons of C4cereal species. J. Exp. Bot. 72(14): 5221–5234. doi: 10.1093/jxb/erab251.

862   Vanderborght, J., V. Couvreur, F. Meunier, A. Schnepf, H. Vereecken, et al. 2021. From hydraulic root
863   architecture models to macroscopic representations of root hydraulics in soil water flow and land
864   surface models. Hydrol. Earth Syst. Sci. 25(9): 4835–4860. doi: 10.5194/hess-25-4835-2021.

865   Vanderborght, J., A. Graf, C. Steenpass, B. Scharnagl, N. Prolingheuer, et al. 2010. Within-Field Variability
866   of Bare Soil Evapora Ө on Derived from Eddy Covariance Measurements. Vadose Zo. J. 9: 943–954.
867   doi: 10.2136/vzj2009.0159.

868   Vereecken, H., A. Schnepf, J.W. Hopmans, M. Javaux, D. Or, et al. 2016. Modeling Soil Processes: Review,
869   Key Challenges, and New Perspectives. Vadose Zo. J. 15(5): vzj2015.09.0131. doi:
870   10.2136/vzj2015.09.0131.

871   Vetterlein, D., M. Phalempin, E. Lippold, S. Schlüter, S. Schreiter, et al. 2022. Root hairs matter at field
872   scale for maize shoot growth and nutrient uptake, but root trait plasticity is primarily triggered by
873   texture and drought. Plant Soil 478(1–2): 119–141. doi: 10.1007/s11104-022-05434-0.

874   Vitale, L., P. Di Tommasi, C. Arena, A. Fierro, A. Virzo De Santo, et al. 2007. Effects of water stress on gas
875   exchange of field grown Zea mays L. in Southern Italy: An analysis at canopy and leaf level. Acta
876   Physiol. Plant. 29(4): 317–326. doi: 10.1007/s11738-007-0041-6.

877   Wang, N., J. Gao, and S. Zhang. 2017. Overcompensation or limitation to photosynthesis and root hydraulic
878   conductance altered by rehydration in seedlings of sorghum and maize. Crop J. 5(4): 337–344. doi:

879   10.1016/j.cj.2017.01.005.

880 Weihermüller, L., Huisman, J. A., Lambot, S., Herbst, M., & Vereecken, H. (2007). Mapping the spatial
881   variation of soil water content at the field scale with different ground penetrating radar techniques.
882   Journal of Hydrology, 340, 205–216. https://doi.org/10.1016/j.jhydrol.2007. 04.013

883 Welcker, C., W. Sadok, G. Dignat, M. Renault, S. Salvi, et al. 2011. A common genetic determinism for
884   sensitivities to soil water deficit and evaporative demand: Meta-analysis of quantitative trait loci and
885   introgression lines of maize. Plant Physiol. 157(2): 718–729. doi: 10.1104/pp.111.176479.

886 Zhuang, J., Y. Jin, and T. Miyazaki. 2001. ESTIMATING WATER RETENTION CHARACTERISTIC FROM SOIL
887   PARTICLE-SIZE DISTRIBUTION USING A NON-SIMILAR MEDIA CONCEPT. Soil Sci. 166(5).
888   https://journals.lww.com/soilsci/Fulltext/2001/05000/ESTIMATING_WATER_RETENTION_CHARACT
889   ERISTIC_FROM.2.aspx.

890 Zwieniecki, M.A., P.J. Melcher, C.K. Boyce, L. Sack, and N.M. Holbrook. 2002. Hydraulic architecture of leaf
891   venation in Laurus nobilis L. Plant, Cell Environ. 25(11): 1445–1450. doi: 10.1046/j.1365-
892   3040.2002.00922.x.

893

Author contribution

895 Huu Thuy Nguyen, Thomas Gaiser, Jan Vanderborght, and Frank Ewert: Conceptualization; Huu Thuy

896 Nguyen, and Hubert Hüging: Data curation and data quality check (aboveground measurements); Lena

897 Lärm, Felix Bauer, Anja Klotzsche, Jan Vanderborght, and Andrea Schnepf: data curation and data quality

898 check (belowground measurements); Huu Thuy Nguyen: Formal data analysis and visualization; Thomas

899 Gaiser, Jan Vanderborght, Andrea Schnepf, and Frank Ewert: Funding acquisition & Project administration;

900 Huu Thuy Nguyen: writing – original draft; all authors: review, editing, and finalizing the manuscript.

Competing interests

902 This manuscript has not been published and is not under consideration for publication in any other journal.

903 All authors agreed and approved the manuscript and its submission to this journal. We declare there is no

904 conflict of interest.

Code/Data availability

906 The meteorological data were collected from a weather station in Selhausen (Germany) which belongs to

907 the TERENO network of terrestrial observatories. Weather data are freely available from the TERENO data

908 portal (https://www.tereno.net/ddp/dispatch?searchparams=freetext-Selhausen, last access:

909 October 2020) (TERENO, 2020). The data which were obtained from the minirhizotron facilities (under-

910 and aboveground) are publicly available in Lärm et al., (2023) and in Nguyen et al., (2024), respectively.

List of Tables

Table 1. Crop phenology and management information for different treatments in 2017 and 2018.

	2017				2018			
Soil types	Stony (F1)	Stony (F1)	Silty (F2)	Silty (F2)	Stony (F1)	Stony (F1)	Silty (F2)	Silty (F2)
Water treatments	Rainfed (P2)	Irrigated (P3)	Rainfed (P2)	Irrigated (P3)	Rainfed (P2)	Irrigated (P3)	Rainfed (P2)	Irrigated (P3)
Plot names	F1P2	F1P3	F2P2	F2P3	F1P2	F1P3	F2P2	F2P3
Growing season (days)$^{¥}$	136	136	136	136	107	107	107	107
Cumulative rainfall (mm)[*]	248.7	248.7	248.7	248.7	91.3	91.3	91.3	91.3
Irrigation (mm)	0	130	0	130	66	257.6	0	257.6
Fertilizer application (mm/dd) (per hectare)	05/09:100 kg N + 40kg P_2O_5 07/06: 80 kg N + 40 kg K_2O				05/22: 100 kg N 05/30: 40 kg P_2O_5 + 40 kg K_2O 06/27: 80 kg N			
Sowing date (mm/dd)	05/04				05/08			
Emergence date	05/09				05/13			
Tasseling date	07/09				07/09			
Silking date	07/14				07/11			
Harvest date	09/12				08/22			

Notes: [¥] from sowing to harvest; [*] for rainfall for whole growing season;
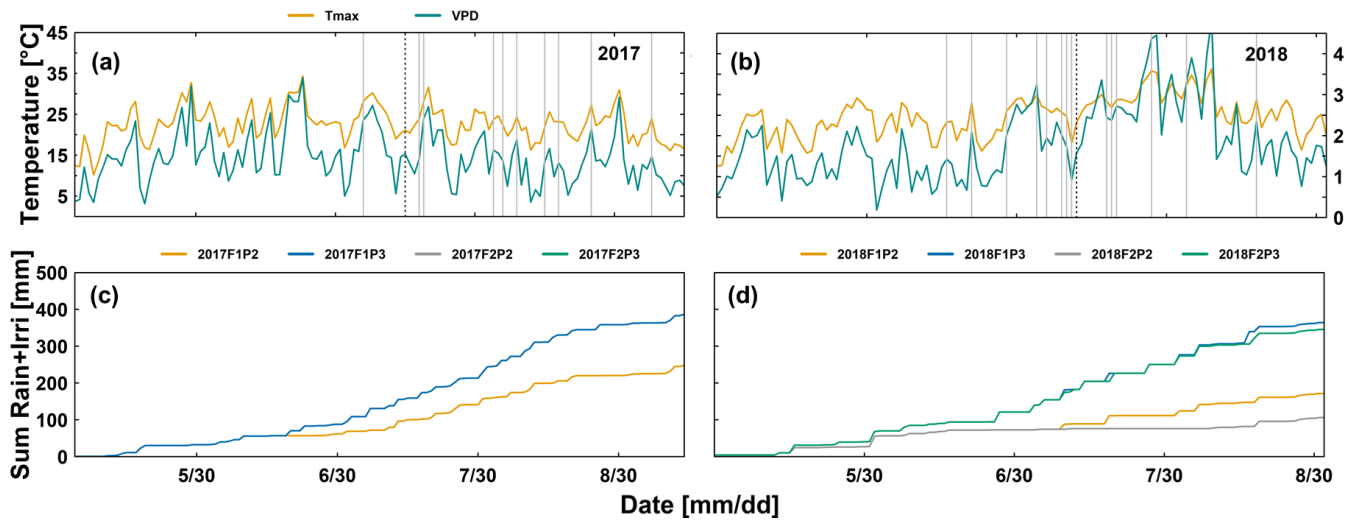
Figure 1: Daily maximum air temperature (Tmax) (°C), daily maximum air vapor pressure deficit (VPD) (kPa) in the two growing seasons (a) 2017 and (b) 2018 and cumulative (sum) of rainfall and irrigation from the rainfed (P2) and irrigated (P3) plots of the stony soil (F1) and silty soil (F2) in the two growing seasons (c) 2017 and (d) 2018. The black dashed vertical lines (a) and (b) indicate silking time. Grey vertical lines in (a) and (b) indicate the measured days for leaf gas exchange and leaf water potential. Two lines for 2017F2P2 and 2017F2P3 were overlapped by the lines from 2017F1P2 and 2017F1P3, respectively
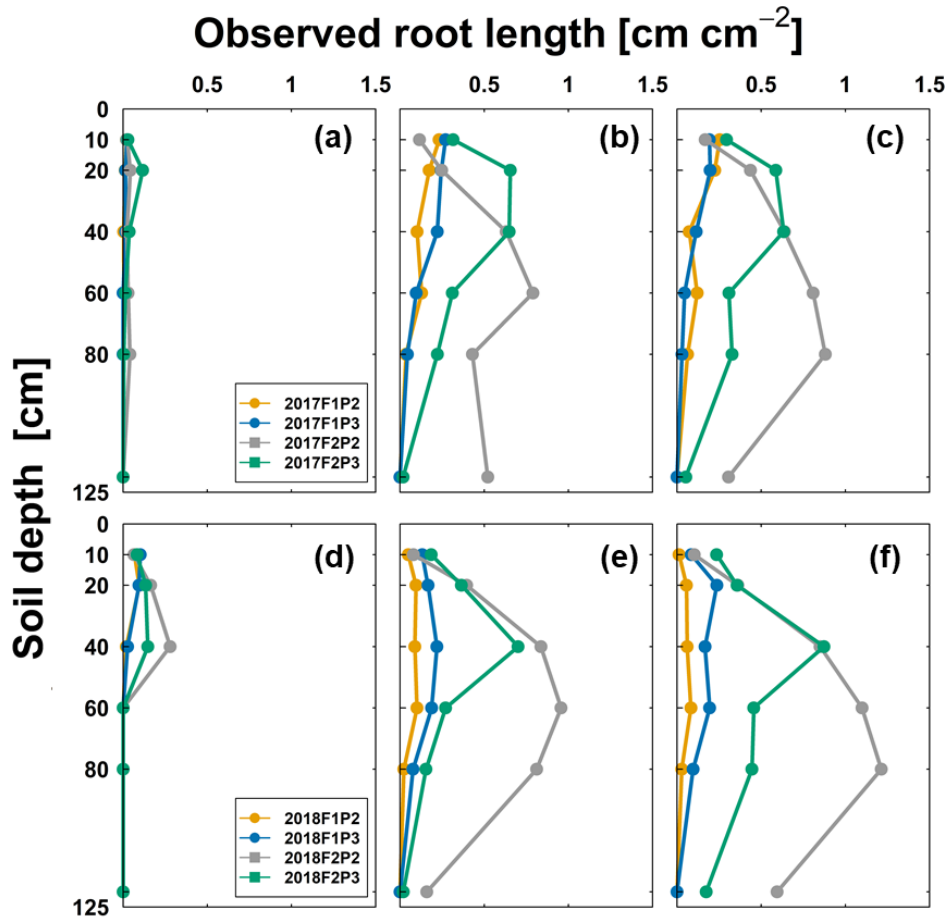
Figure 2: Observed root length from minirhizotubes (cm cm^{-2}) from 10, 20, 40, 60, 80, and 120 cm soil depth from the rainfed (P2) and irrigated (P3) plots of the stony soil (F1) and silty soil (F2) in the two growing seasons in 2017 (a - 8 June, b - at silking on 13 July, c - at harvest on 12 September) and in 2018 (d - 7 June, e - at one week after silking - 18 July, f - one week before harvest - 16 August).
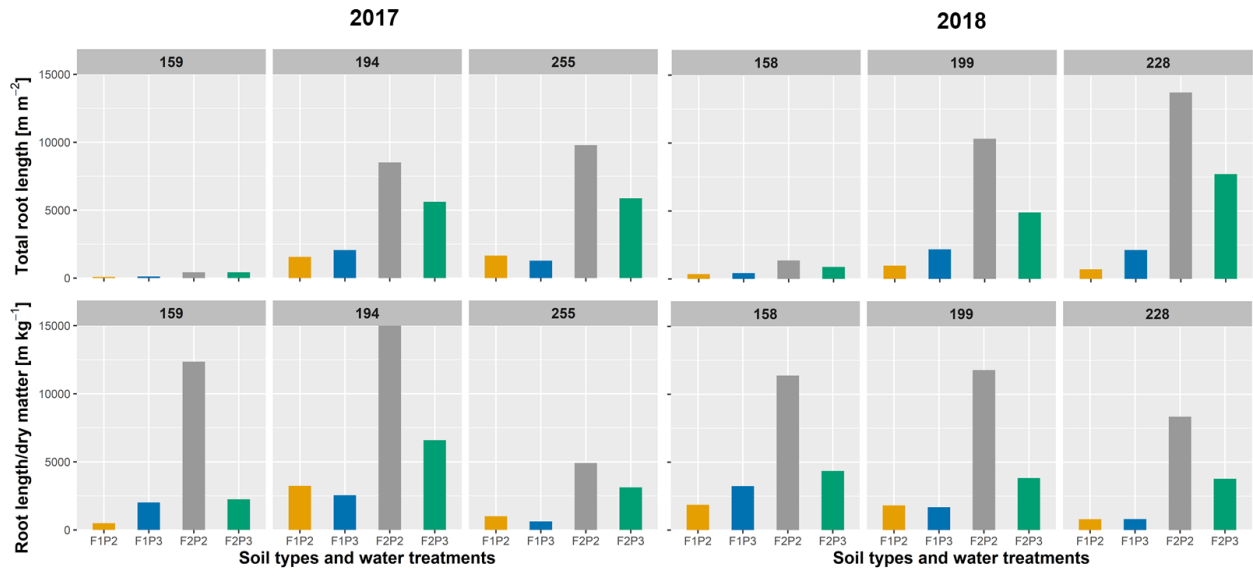
Figure 3: Observed root length from minirhizotubes (m m⁻²) and ratio of root length per shoot dry matter (m kg⁻¹) from the rainfed (P2) and irrigated (P3) plots of the stony soil (F1) and silty soil (F2) in the two growing seasons (DOY 159, 194, and 255, left panel) in 2017 and in 2018 (DOY 158, 199, and 228, right panel) where on 8 June (DOY 159) at silking on 13 July (DOY194) 2017; and at harvest on 12 September (DOY 255) in 2017; 7 June (DOY 158), one week after silking on 18 July (DOY 199); and one week before harvest on 16 August (DOY 228) in 2018 (see also Figure 2).
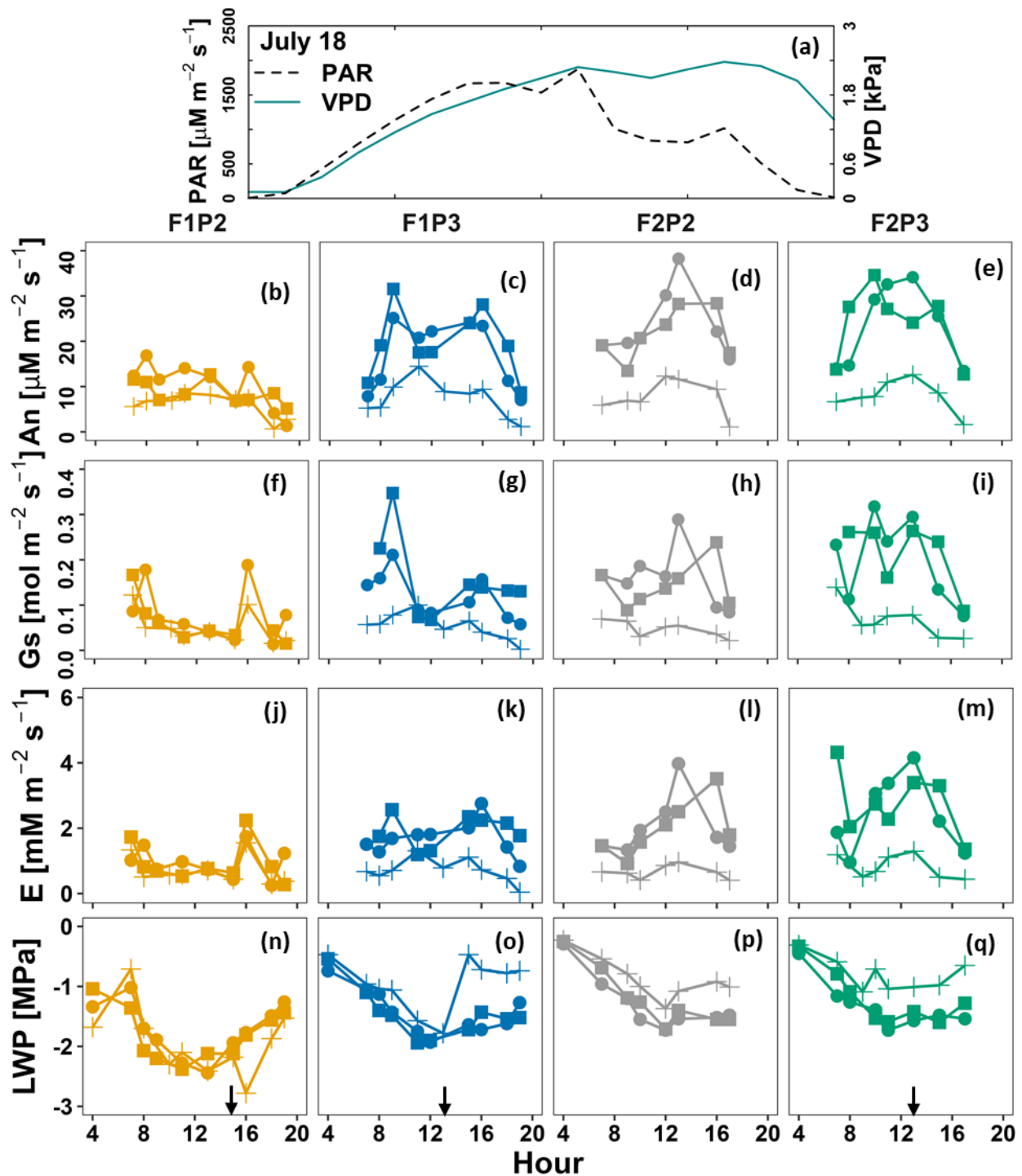
Figure 4. Diurnal course of (a) photosynthetically active radiation (PAR) and vapor pressure deficit (VPD), (b –e) leaf net photosynthesis (An), (f –i) leaf stomatal conductance (Gs), (j –m) leaf transpiration (E), and (n –q) leaf water potential (LWP) on 18 July in maize in 2018 before irrigation at the rainfed (P2) and irrigated (P3) plots of the stony soil (F1) and silty soil (F2). Measurement was carried out from shaded leaf (plus symbol with line) and two sunlit leaves (solid dot - lines and solid square - lines). Crop was irrigated at 1 PM, 1 PM, 4 PM for F1P3, F2P3, and F1P2, respectively (22.75 mm for each plot) (Supp. 2). Black arrows indicate time of irrigation.
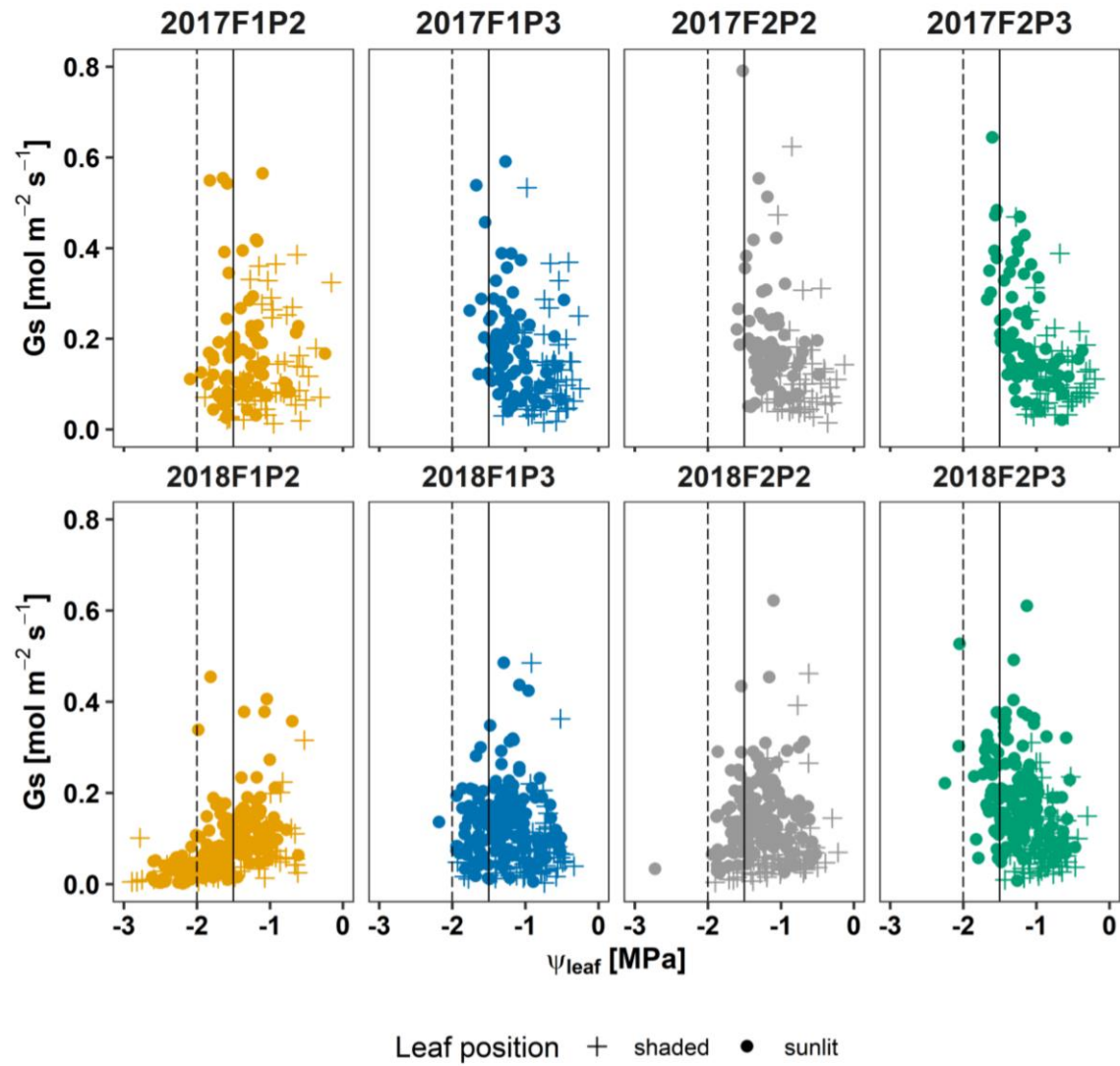
Figure 5: Seasonal stomatal conductance to water vapor (Gs) versus leaf water potential (ψ_{leaf}) in 2017 (top panel) and in 2018 (bottom panel) at the rainfed (P2) and irrigated (P3) plots of the stony soil (F1) and silty soil (F2). Vertically continuous and dashed lines indicated ψ_{leaf} at -1.5 and -2 MPa, respectively. Measurement was carried out from shaded leaf (plus symbol) and two sunlit leaves (solid dots)
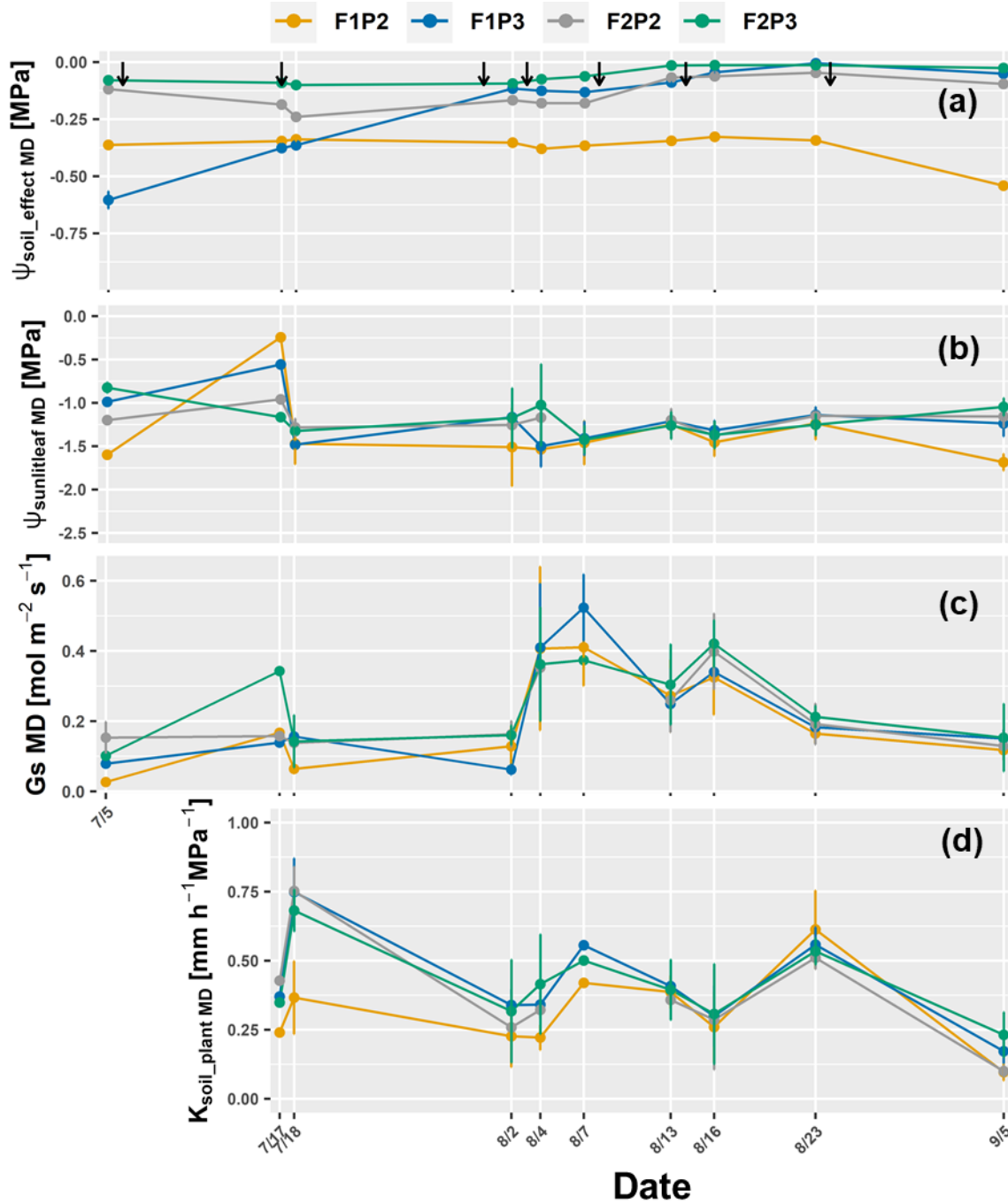
Figure 6: Dynamic of around midday (MD) of (a) the effective soil water potential ($\psi_{soil\_effec, MD}$) (b) sunlit leaf water potential ($\psi_{sunlitleaf\ MD}$), (c) stomatal conductance (Gs MD) and (d) whole soil-plant hydraulic conductance ($K_{soil\_plant\ MD}$) in the growing season 2017 from the rainfed (P2) and irrigated (P3) plots of the stony soil (F1) and silty soil (F2). Error bars indicate the standard deviation of the different values taken around midday (11 AM, 12AM, 1PM, and 2 PM) of different sunlit leaves. Whole soil-plant hydraulic conductance was shown from 17 July when sap flow was measured. The black arrows indicates the irrigation events for the irrigated treatments F1P3 and F2P3 in the showing period.
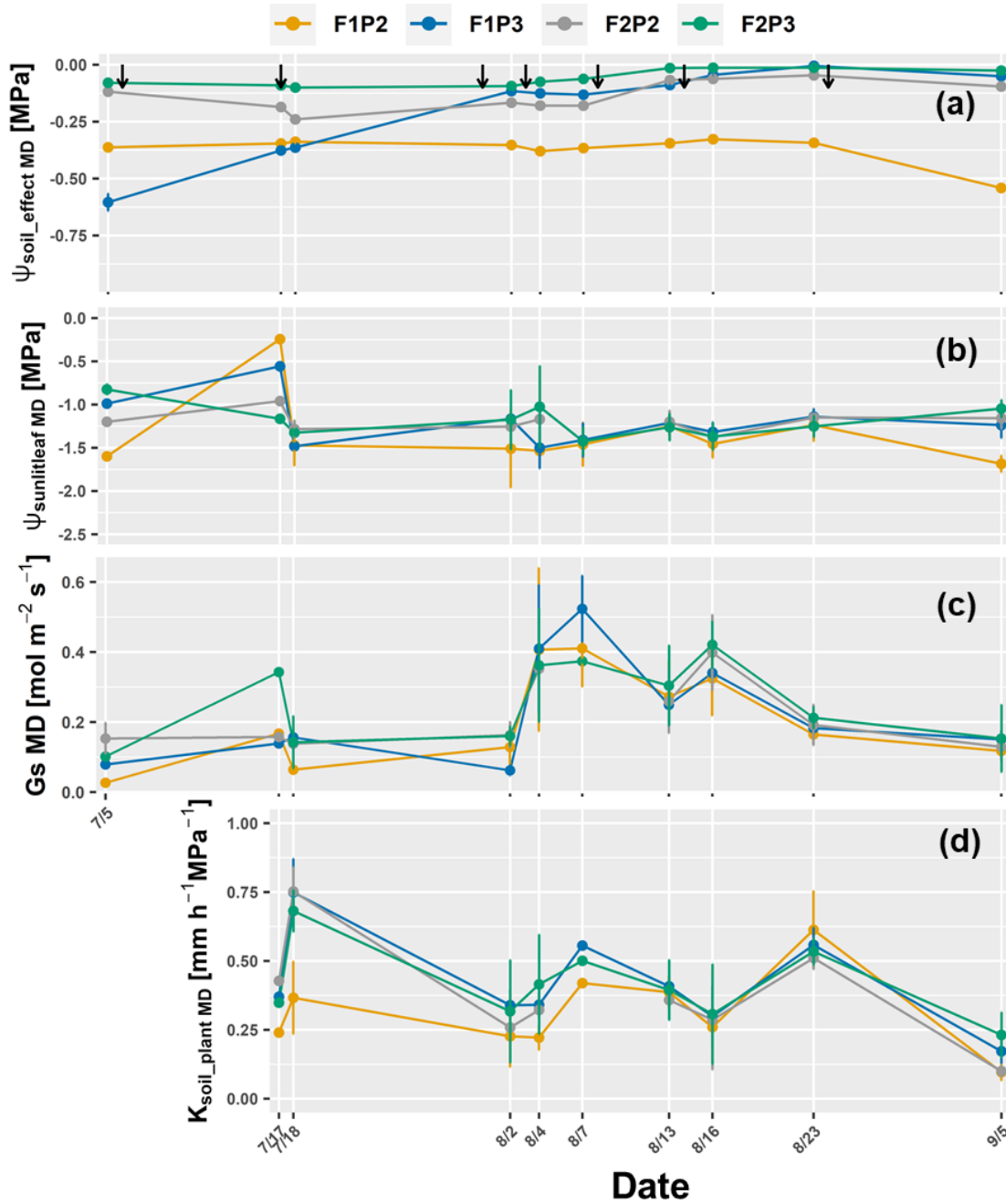
Figure 7: Dynamic of around midday (MD) of (a) the effective soil water potential ($\psi_{soil\_effec\ MD}$) (b) sunlit leaf water potential ($\psi_{sunlitleaf\ MD}$), (c) stomatal conductance (Gs MD) and (d) whole soil-plant hydraulic conductance ($K_{soil\_plant\ MD}$) in the growing season 2018 from the rainfed (P2) and irrigated (P3) plots of the stony soil (F1) and silty soil (F2). Error bars indicate the standard deviation of the different values taken around midday (11 AM, 12AM, 1PM, and 2 PM) Leaf water potential and stomatal conductance were 2 sunlit leaves and one shaded leaf at each measured hour. Whole soil-plant hydraulic conductance was shown from 3 July when sap flow was measured. The black arrows indicates the irrigation events for the irrigated treatments F1P3 and F2P3 while the orange arrow indicates the irrigation application for the rainfed plot at the stony soil (F1P2).
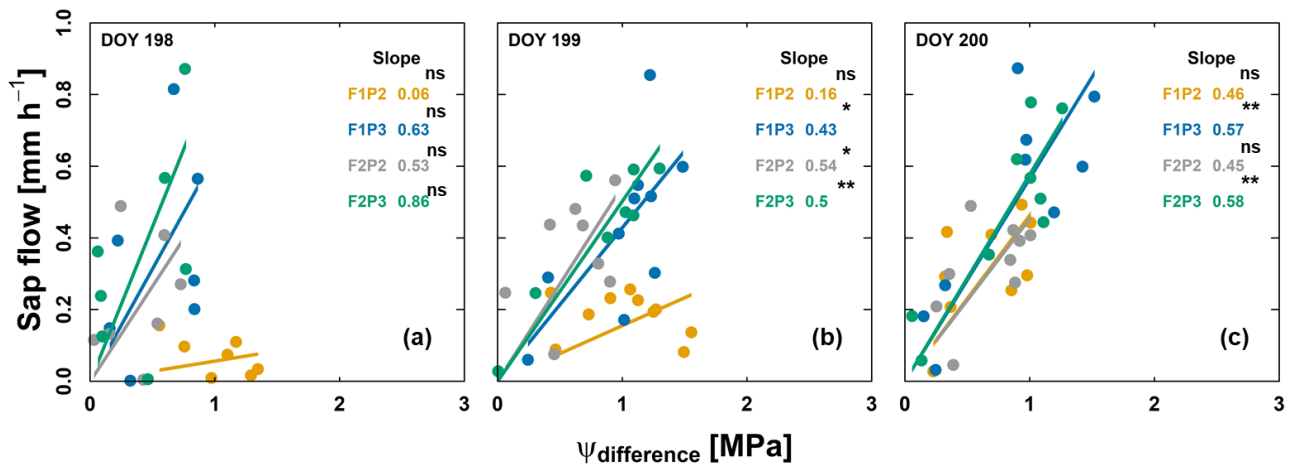
Figure 8: Relationship of sap flow and difference of effective soil water potential and sunlit leaf water potential ($\psi_{difference}$) from the rainfed (P2) and irrigated (P3) plots of the stony soil (F1) and silty soil (F2) on three consecutive measurement days from predawn in 2018 (a) 17 July - DOY 198, (b) 18 July - DOY 199 and (c) 19 July - DOY 200. Crop was irrigated on 18 July (DOY 199) at 1 PM, 1 PM, and 4 PM for F1P3, F2P3, and F1P2, respectively (22.75 mm for each plot). The unit of slope in the linear regression (or soil-plant hydraulic conductance) is mm h^{-1} MPa^{-1}. Regression was based on the DEMING approach. The asterisk which are next to the slopes indicate a significant correlation between two variables according to Pearson method (ns: non-significant; * $p < 0.05$; ** $p < 0.01$; *** $p < 0.001$).
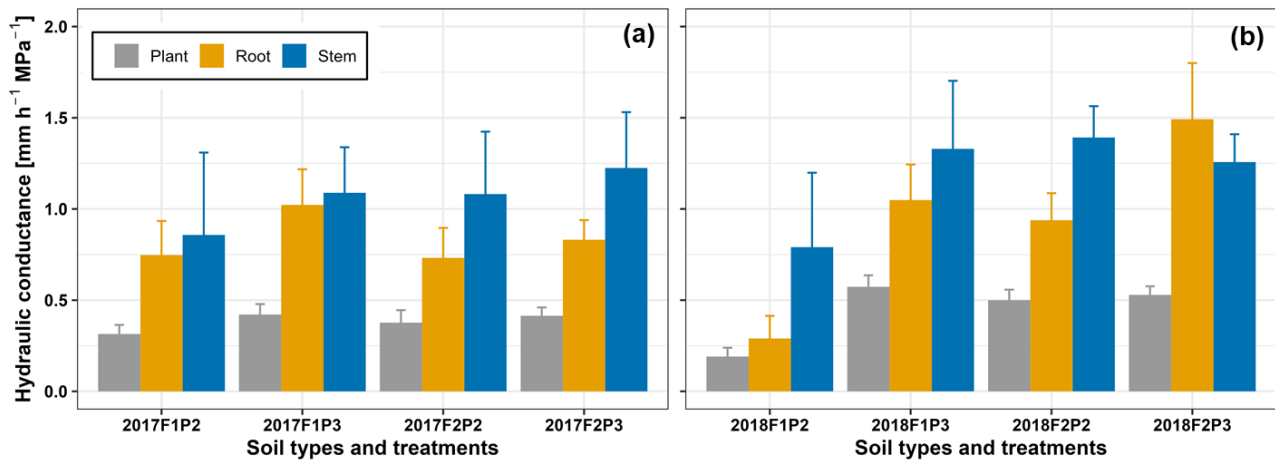
Figure 9: Comparison of different midday hydraulic components (mm h^{-1} MPa^{-1}): soil-plant (grey bars), soil-root (yellow bars), and stem (blue bars) from the rainfed (P2) and irrigated (P3) plots of the stony soil (F1) and silty soil (F2) in the two growing seasons (a) in 2017 and (b) in 2018. The error bars indicate the standard deviation from measurements around midday (11 AM, 12AM, 1PM, and 2 PM) in different measured days (in 2017 with n = 4 x 9 days, Supplementary material 10, 11, and Fig. 6 and in 2018 with n = 4 x 10 days, Supplementary material 10, 12, and Fig. 7).
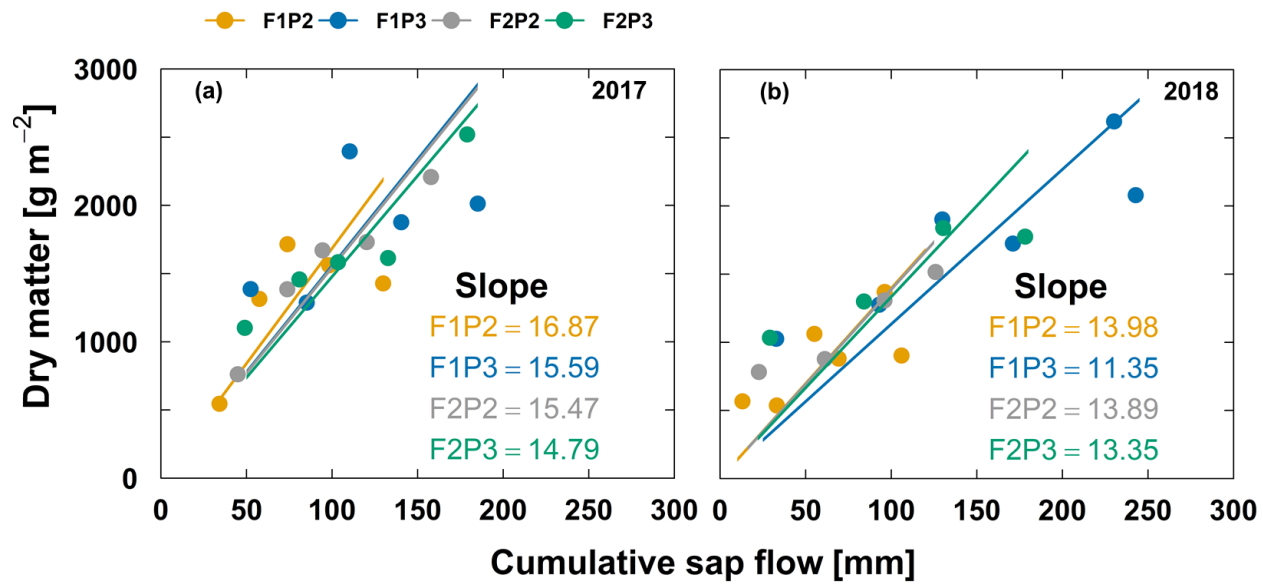
Figure 10: Relationship of aboveground dry matter and cumulative sap flow from the rainfed (P2) and irrigated (P3) plots of the stony soil (F1) and silty soil (F2) in the two growing seasons (a) 2017 and (b) 2018. The unit of slope linear relationship is g mm^{-1}. The less number of data points in (b) in 2018 from the F2P2 and F2P3 plots were due to the missing values of measured sap flow because of sensor disconnection. For aboveground dry matter, each point represents the average of two sampling replicates, except the harvest with 5 sampling replicates.